Characterization of regulatory proteins within the Pak2 signaling pathway on prostate cancer migration

by

© Ricardo Carmona Martínez

A Thesis submitted to the

School of Graduate Studies

In partial fulfillment of the requirements for the degree of

Master of Science (Medicine)

Cancer and Development Program

Division of Biomedical Sciences

Faculty of Medicine

Memorial University of Newfoundland

May, 2017

St. John's Newfoundland and Labrador

Abstract

Prostate cancer is the most frequently diagnosed cancer among men, with an incidence rate of 1 in 7. The mechanisms regulating its abnormal growth and metastasis are not fully understood. Transforming Growth Factor-Beta (TGF-β) has been described as both a negative prognostic indicator and a growth promoter in prostate cancer. The p21-Activated kinase 2 (Pak2) enzyme regulates growth and migration of normal cells and has been shown to be activated by TGF-β. My hypothesis proposes that Pak2 regulates the aberrant migratory properties of prostate cancer. Multiple prostate cancer cell lines, representing multiple stages in disease development were used to define protein and gene expression levels within the Pak2 signaling cascade. P-Merlin levels were used to determine Pak2 activity. There is a shift in the ratio of Pak2 stimulatory proteins with a dominance of CDC42 corresponding with disease progression. The ratio of Merlin to Erbin is altered in all prostate cancer cells. There is an increase in P-Merlin levels corresponding to progression of the disease, indicating an increase in basal Pak2 activity. Pak2 inhibition blocked TGF-β promoted migration in highly metastatic prostate cancer cells PC-3 and DU145. These results demonstrate the Pak2 signaling pathway is not only aberrantly active but that regulates TGF-β induced migration in prostate cancer.

Acknowledgements

I would like to express my sincere gratitude and respect to my supervisor Dr. Jules Dore for giving me the opportunity to work in his lab, for his constant support, teachings and valuable discussions which made it possible for me to get an excellent lab experience and complete the following thesis.

I would like to thank the rest of my thesis committee: Dr. Ken Kao and Dr. John Thoms for their helpful comments, time and support.

I would like to express my gratitude to my partner, Paola Gonzalez, for her unconditional love, support and help during stressful times and her invaluable advice that helped me get thought the program. I also thank my mother Araceli M.; my sister Araceli C.; my grandmother Silvia M. and my extended family Mauricio G. for their support during the program.

Table of Contents

List of Tables

List of Figures

List of Symbols, Nomenclature or Abbreviations

^{0} C – Celsius

μl - Microliter

ΔΔCt - Relative quantitative comparison cycle threshold

AKT – Protein kinase B

ANOVA – Analysis of variants

ATTC - American Type Culture Collection

BCA - Bicinchoninic acid

BPE - Bovine pituitary extract

CD44 – Cell surface marker

CD57 - Cluster of Differentiation 57

CDC42 - Cell division control protein 42

cDNA – Complementary DNA

DNA - Deoxyribonucleic acid

DOC - Deoxycholic Acid

DMSO – Dimethyl sulfoxide

EDTA - Ethylenediaminetetraacetic acid

EGF - Epidermal growth factor

EMT - Epithelial to mesenchymal transition

Erbin – Erbb2 interacting protein

ERM – (ezrin, radixin, and moesin) family

ERK – Extracellular signal regulated kinase

FBS - Fetal bovine serum

FGF – Fibroblast growth factor

GSK-3β – Glycogen synthase kinase 3 beta

HGF – Hepatocyte growth factor

IgG - Immunoglobulin G

JNK - c-Jun N-terminal kinases

K-SFM - Keratinocyte serum free medium

LAP – Leucine-rich repeats and PDZ domain

mM – Millimolar

mg - Milligram

MKNK1 - MAPK-interacting serine/threonine protein kinase 1

ml - Milliliter

NaF - Sodium Fluoride

NF2 - Neurofibromatosis type 2

P63 – homologo of p53

Pak - P21 activated kinase

Pak2 - P21 activated kinase 2

PBS - Phosphate-Buffered Saline

PCR - Polymerase chain reaction

PDB - P21-binding domain

PDZ – Acronym of the first proteins were the domain was found (PSD-95; Dlg1; ZO-1)

P-ERK – Phospho-p44/42 (Thr202/TYR204) ERK

P-GSK-3β – Phospho-GSK-3β

PI3K – Phosphatidylinositol 3-kinases

PIN – Prostatic intraepithelial neoplasia

P-Merlin – Phospho-Merlin

PMSF - Phenylmethylsulfonyl fluoride

PSA - Prostate-specific antigen

PVDF - Polyvinyl difluoride

qPCR – Quantitative PCR

RIPA - Radio-Immunoprecipitation Assay

RNA – Ribonucleic acid

RT - Reverse Transcription

SDS - Sodium Dodecyl Sulfate

TBST - Tris-buffered saline Tween

TGFβRI - Transforming Growth Factor β receptor I

TGFβRII - Transforming Growth Factor β receptor II

TGF-β - Transforming Growth Factor β

TRIS-HCl - Tris-Hydrochloride

Chapter I - Introduction

1.1 Prostate Cancer Statistics

Prostate cancer is the second most common cancer affecting men worldwide, especially in western developed countries. The incidence of prostate cancer diagnosis varies around the world, Caribbean men have a 26% risk of being diagnosed by the age of 74 years old, while in Asia the risk is 0.15%, indicating that ethnicity may play a role in prostate cancer incidence (Canadian Cancer Society's Advisory Committee on Cancer Statistics, 2015). Prostate cancer mortality falls to second place only to lung cancer deaths worldwide. According to the Canadian Cancer Society, one in seven Canadian men are expected to be diagnosed with prostate cancer in their life time. Approximately 24,000 new cases are expected per year in Canada, representing 24% of all new male cancer cases. In the United States, prostate cancer has become the second leading cancer in males (in new cases and deaths) representing 27% of all new cancer cases. Prostate cancer is more commonly diagnosed in males between 60 to 69 years old. As men get older the risk of developing prostate cancer increases (Canadian Cancer Society's Advisory Committee on Cancer Statistics, 2015; Hodson, 2015; Siegel et al., 2014).

Prostate cancer accounts for the majority of bone metastases diagnosed in men in the USA. Studies utilizing large databases found that 7.7 % of men with prostate cancer had evidence of bone metastasis at diagnosis. These men were more likely to be older than a matched cohort of men without bone metastasis with a median age of 76 versus 74 (Brawley, 2012). Race and comorbidity do not appear to influence the risk of presenting bone metastasis at diagnosis. The risk of death is 6.6 fold higher for those with bone metastasis and no evidence of skeletal-related events at presentation compared to those without bone metastases (Sathiakumar et al.,

2011). When both bone metastasis and skeletal-related events are present at diagnosis, the death risk increases to 10.2 fold (Bubendorf et al., 2000).

1.2 The Prostate Gland

The prostate is an exocrine gland considered to be slightly bigger than a walnut, about 3 centimeters in length weighting approximately 20 grams. It is located underneath the bladder, surrounding the urethra. The gland's principal function is to produce, store and secrete seminal fluid components (Huggins et al., 1942). The prostate was first described as a gland composed of 3 zones by McNeal (*Figure 1.1*); the transitional zone, the central zone and the peripheral zone (the largest zone), the origin of 70 to 80% of prostate carcinomas (McNeal, 1969; Myers, 2000).

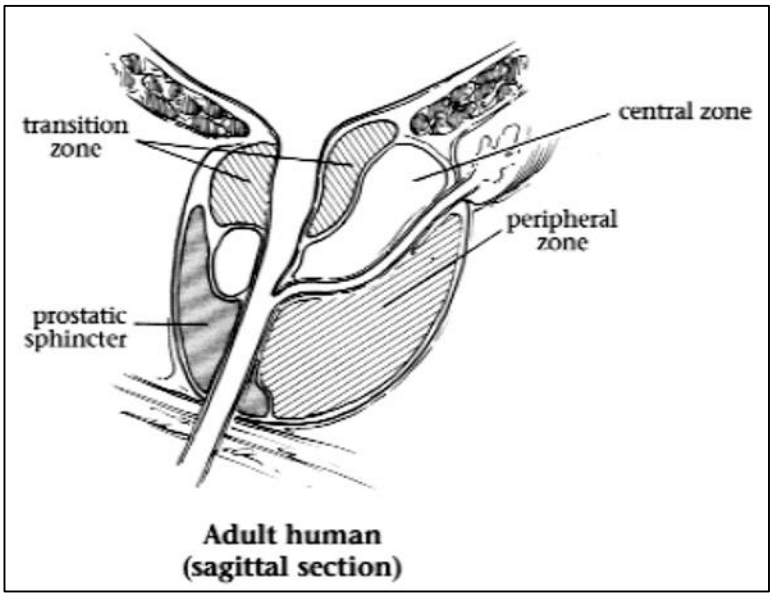

Figure 1. 1 – Anatomy of a normal human prostate gland. Used with permission Cold Spring Harbor Laboratory Press, Abate-Shen (2000)

There are three main epithelial cell types identified in the normal prostate: the basal, luminal, and neuroendocrine cells (*Figure 1.2*). The neuroendocrine cells do not express androgen receptor, making them androgen independent cells. Their exact role and function is unclear, but it is established that they have a role in the growth and differentiation of the prostate and therefore, implicated in carcinogenesis. Neuroendocrine cells are characterized by the expression of chromogranin A, serotonin, synaptophysin and neuro specific enolase (NSE). The basal layer is considered to be the proliferative compartment of the prostate and its cells express p63, cytokeratins 5 and 14, and the cell surface marker CD44. The luminal layer consists of androgen dependent cells. The androgen receptor is present in luminal cells which also express the cytokeratins 8 and 18, and the cell surface marker CD57 (Abate-Shen and Shen, 2000; Long et al., 2005; Vashchenko N and Abrahamsson PA, 2005). Additionally, the luminal cells are the source of kallikrein 3, also known as the prostate specific antigen (PSA; Lilja et al., 1987).

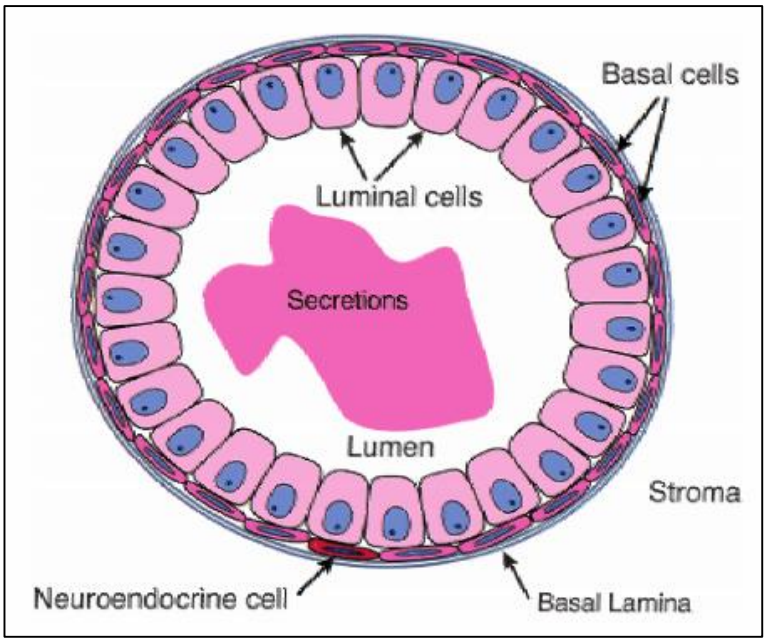

Figure 1. 2 - The three differentiated cell types in the prostate epithelium. Used with permission Cold Spring Harbor Laboratory Press Abate-Shen (2000)

1.3 Initiation and Progression of Prostate Cancer

Through the development of prostate cancer studies, scientists believe that prostatic intraepithelial neoplasia (PIN), are the precursor of prostate cancer. Reports suggest a transition exists between atrophic epithelium and adenocarcinoma in which areas with chronic inflammation and a high grade PIN present signs of oxidative stress, genetic instability and a cluster of inflammation (Marzo et al., 2007; Weir, 2015). There are two different types of PIN, low grade and high grade, however, the term PIN is commonly applied to indicate the high-grade form. PIN is typically characterised by a drastic reduction in the basal cell population, and exponential increase in luminal cells. These luminal cells develop alterations in their structure resulting in the loss of adhesion and changes in their cytoskeleton. PIN progression into adenocarcinoma is attributed to the inactivation of tumor suppressors and the activation of oncogenes. Adenocarcinoma is generally recognized by the absence of basal cells and extensive proliferation of altered luminal cells. These luminal cells have changed their structure, motility, proliferation and gained invasive properties that permit them to metastasize throughout the body (Abate-Shen and Shen, 2000; Bostwick, 2000; *Figure 1.3*). In a process referred to as epithelial to mesenchymal transition (EMT), epithelial cells lose their cell polarity and cell-cell adhesion, gaining migratory and invasive properties similar to mesenchymal cells.

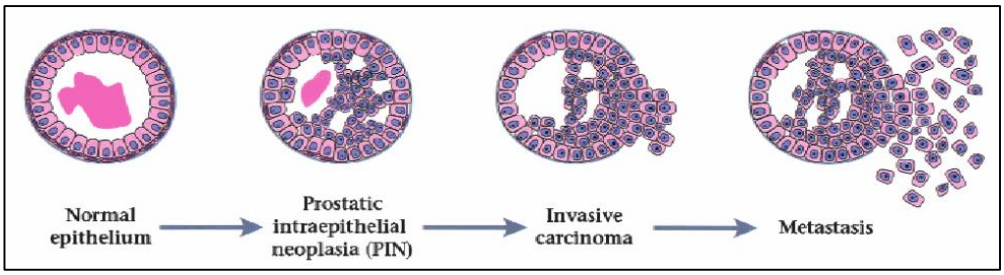

Figure 1. 3 - Progression of prostate cancer. Used with permission Cold Spring Harbor Laboratory Press Abate-Shen (2000)

Epithelial to mesenchymal transition (EMT) is commonly associated with cancer migration, invasion and metastasis. EMT is normally a highly conserved embryonic program where polarized immobile epithelial cells transition to motile, mesenchymal-like cells (Greenburg and Hay, 1982). During development, this process is reversible in morphology ending with a process called mesenchymal to epithelial transition or MET. In contrast, cancer cells having already acquired EMT, subsequently undergoing MET leads to acquiring a more aggressive phenotype rather than a less aggressive one (Yates et al., 2007).

The canonical mediators of EMT during embryogenesis are members of the TGF-β superfamily and the WNT family (Yang and Weinberg, 2008). The common characteristic of EMT is the loss of E-cadherin, associated with decreased cell-cell adhesion, and an increase in Vimentin, a major cytoskeletal component of mesenchymal cells. In cancer, EMT is thought to allow benign tumors to infiltrate surrounding tissues and metastasize (Xu et al., 2006).

Due to the EMT molecular alterations, prostate cancer cells become detached at the invasive tumor front, migrating out of the tumor cell clusters and traveling through the lymph-vascular system to metastasize typically to the bone (Vleminckx et al., 1991). The prostate cancer metastatic tumor cells interact with growth factors that are produced in or released from the bone microenvironment, which plays a crucial role in stimulating bone colonization (Buijs and van der Pluijm, 2009; Buijs et al., 2007). Bone metastases occur in more than 90% of patients with advanced prostate cancer and a high burden of metastatic disease is associated with poor survival (Carlin and Andriole, 2000). In the bone microenvironment, prostate cancer metastatic cells acquire osteoblastic properties through independent activation of the Notch signaling pathway promoting angiogenesis. (Zayzafoon et al., 2004). Additionally, growth factors and alterations in signalling pathways such as TGF-β, epidermal growth factor (EGF),

hepatocyte growth factor (HGF), fibroblast growth factor (FGF), and hypoxia, Snail, and Slug play prominent roles in EMT induction of the primary tumor and have been identified as important stimulators of skeletal metastasis formation (Papachristou and Basdra, 2012).

1.4 Prostate Cancer Diagnosis

Prostate cancer mortality rates have been decreasing since early 2000, this can be attributed to improved treatments and the introduction of the frequency of prostate-specific antigen (PSA) testing for its detection (Siegel et al., 2014; Siegel et al., 2015). PSA expression has been commonly applied as the main tool for prostate cancer detection; it screens for high levels of PSA in the blood enabling early detection of prostate cancer. However, an elevated reading is not necessarily due to a malignant tumor, mistakenly labelling many men who do not have cancer. The US National Cancer Institute estimates that for every 1,000 men screened regularly with the PSA test over the course of a decade, as many as 120 will get a false-positive result, while 110 will get an appropriate positive diagnosis (Sohn, 2015).

Metastatic prostate cancer is commonly fatal and unfortunately existing therapies do not substantially increase survival. Over 80% of patients show a positive response to androgen deprivation therapy. However, patients with metastatic prostate cancer eventually experience disease progression after androgen deprivation therapy. The principal reason for the inability of the androgen deprivation therapy to successfully increase survival in men with metastatic prostatic cancer is that the cancer within each individual patients can be heterogeneously composed of both androgen dependent and independent prostate cancer cells in these particular patients. This heterogeneous state is present even before the therapy is initiated, making the

therapy ineffective on the pre-existing androgen independent cells (Heinlein and Chang, 2004; Kyprianou et al., 1990).

While early detection of prostate cancer is important for diagnosis and prognosis, the main concern is distinguishing between the aggressive and the indolent forms of the disease. Once the cancer starts to spread to the nearby lymph nodes, bone or visceral organs; the 5 year estimated survival rate drops to 28% (Deweerdt, 2015; Stattin et al., 2015). For the indolent form active surveillance is selected when physicians consider men to have a low risk of disease progression after results from the diagnosis with their Gleason score, clinical stage of the cancer progression and their PSA levels (Wadman, 2015).

1.5 Transforming Growth Factor β

Transforming Growth Factor β (TGF-β) is the prototypic member of a family of cytokines that control numerous cellular functions including cell migration, proliferation, differentiation, apoptosis and EMT (Grant and Kyprianou, 2013; Massagué, 2008). TGF-β's (TGF-β1, TGF-β2, and TGF-β3) stimulate the cellular response through the TGF-β type I (TGFβRI) and type II (TGFβRII) receptor signalling complex. Binding of TGF-β to the receptor complex induces signal transduction resulting in the activation and phosphorylation of transcription factors known as smad2 and smad3 (Franzén et al., 1993; Lin et al., 1992). Activation of smad2 and smad3 results in their interaction with a common mediator smad4 forming an oligomeric complex. This complex is translocated to the nucleus, where it interacts with myriad transcriptional co-regulators and other factors that help in the regulation of target gene expression elicited by TGF-β (Macías-Silva et al., 1996; Zhang et al., 1996). Both epithelial and mesenchymal cells possess this canonical signaling cascade. However, epithelial cells are

growth inhibited, while mesenchymal cells are growth stimulated by TGF-β, suggesting a difference in the signaling mechanism between cell types.

In normal epithelial cells, TGF-β stops the cell cycle at the G1 stage stopping proliferation, induce differentiation, or promote apoptosis. However, deregulation of TGF-β pathway can lead to various pathological conditions, including cancer. When an epithelial cell is transformed into a cancer cell, components of the TGF-β signalling pathway may be mutated (Pasche, 2001), making it impossible for TGF-β to negatively control cell growth, leading to its proliferation. The surrounding stromal (mesenchymal) cells proliferate, increasing their production of TGF-β. TGF-β acts on the surrounding stromal cells, immune cells, endothelial and smooth-muscle to cells; stimulating angiogenesis and making the cancer cells more invasive (Heldin et al., 2009; Principe et al., 2014).

TGF-β has a complex role in cancer. Initially, it was identified as a tumor suppressor since it inhibits the growth of cells and induces apoptosis (Nguyen and Pollard, 2000). However, at later stages of tumor progression TGF-β acts as a tumor promoter (Xie et al., 2002). At a later stage of the disease, the tumor cells lose their ability to be growth arrested by TGF-β, but retain their ability to undergo EMT, which correlates to increased invasiveness and metastasis (Kingsley et al., 2007). In addition, the suppression of the immune system and stimulation of angiogenesis by TGF-β also contributes to its tumor promoting effects (Massagué, 2008; Moustakas and Heldin, 2007).

Smad pathways are part of the canonical TGF-β signaling pathway, though examples of non-smad pathways activated by TGF-β also exist. These non-smad pathways include the extracellular signal regulated kinase (ERK) pathway (Blanchette et al., 2001; Hough et al., 2012), the c-Jun N-terminal kinases (JNK) pathway (Wang et al., 1997), the Phosphatidylinositol

3-kinases (PI3K) pathway (Wilkes et al., 2005) and the p21 activated kinases 2 (Pak2) pathway (Wilkes et al., 2003), among other pathways (Moustakas and Heldin, 2005).

1.5.1 TGF-β and the PI3K Pathway

Phosphatidylinositol 3 kinase (PI3K) is a family of proteins that phosphorylate the 3'-hydroxyl group on the inositol ring of phosphoinositides on the inner side of the plasma membrane (Vanhaesebroeck and Waterfield, 1999). The PI3K family is divided into three different classes: Class I, Class II, and Class III. The class I are heterodimeric molecules commonly composed of a p85 regulatory and p110 catalytic subunit, primarily responsible for mediating the transduction of signals from growth factors and receptors. There is an exception to this rule in that the p110γ catalytic subunit associates with a p101regulatory subunit as part of the G-Coupled protein signaling cascade. The Class II and III PI3K are different from the Class I in structure and function. A distinct feature of Class II PI3Ks is the C-terminal C2 domain (Leevers et al., 1999). Class I PI3K (referred to as PI3K) is involved in the generation of various lipid effectors resulting in promotion of the phosphorylation of several protein substrates whose activity has been linked to cell growth, cellular differentiation, motility, survival, adhesion, and cytoskeletal organization (Jeong and Kim, 2004; Katso et al., 2001). In TGF-β induced EMT, in particular, PI3K has been shown to activate Snail and Slug through Ras-MAPK. Slug triggers the steps of desmosomal disruption, cell spreading, and partial separation at cell–cell borders, which comprise the first and necessary phase of the EMT process (Savagner et al., 1997).

TGF-β receptors I and II activate the PI3K pathway promoting cell survival and enabling protection from TGF-β -induced apoptosis in kidney visceral epithelial cells (Schiffer et al., 2004). Migratory metastatic breast cancer cells produce large amounts of TGF-β, which in turn

stimulates the PI3K pathway, activating the protein kinase B, also known as AKT, and ERK pathway to enhance their motility (Ueda et al., 2004). In a similar process, mammary epithelial cells transformed by the overexpression of the epithelial growth factor receptor 2 (HER2) display enhanced motility generated by the activation of Rac1 through TGF-β. These examples represent the ability for TGF- β to use smad and non-smad signals to generate morphological responses in the cell (Dumont et al., 2003; Ueda et al., 2004).

1.6 Pak2

The P21 activated kinase (Pak) family are a major downstream effector of the small GTPase Rac1 and cell division control protein 42 (CDC42), which are involved in actin-based cytoskeletal remodeling. The Pak family binds to CDC42 and Rac1 through a GTPase binding domain also known as a CDC42/Rac interactive binding domain (Renkema and Pulkkinen, 2002). There are six human known isoforms of Pak, and they are classified into two subgroups: Group A, includes Pak 1 to 3, and Group B, Pak 4 to 6. Group A has an N-terminal regulatory domain and a carboxyl terminal kinase domain. Group B also has an N-terminal domain and a carboxyl terminal kinase domain, but their GTPase binding domain retains only a 50% similarity with those of the group A, suggesting that group A is the primary target of Rac1/CDC42 activation (Bokoch, 2003; Rane and Minden, 2014).

Studies have shown the ability of TGF-β to promote the activation of the smad independent pathway through specific activation of Pak2. TGF-β activation of Pak2 is a normal process that occurs in mesenchymal cells, but it is not a normal event in epithelial cells. Pak2 activation is necessary for the morphological alterations and proliferative responses induced in mesenchymal cells (Hough et al., 2012; Wilkes et al., 2003). Pak2 has been shown to have both

anti-apoptotic and pro-apoptotic functions making it unique among the Pak isoforms. Pak 2 pro-apoptotic functions are attributed to its ability to phosphorylate caspase 7 (Li et al., 2011) However, Pak2 is cleaved by caspase 3 at late stages of apoptosis. The Pak2 proteolytic fragment mediates phosphorylation of MAPK-interacting serine/threonine protein kinase 1 (MKNK1) promoting apoptosis (Orton et al., 2004) . Group A Paks are the central regulators of CDC42 and Rac GTPase signalling, and are involved in cytoskeletal rearrangements (Van den Broeke et al., 2009).

1.6.1 Pak2 Stimulators Rac1 and CDC42

Rac1, CDC42 and Pak proteins are important for physiological responses to growth factors in normal epithelial cells (Somanath and Byzova, 2009) and are involved in the promotion of invasion and migration in prostate cancer and ovarian cancer cells by regulating microtubule dynamics, adhesion (Goc et al., 2012; Siu et al., 2010).

Rac1 and CDC42 are part of the Rho family of small GTP-binding proteins with a distinct function in actin cytoskeleton organization and regulation of cell motility, including cell adhesion, and cell cycle progression (Takai et al., 2001). For instance, Rac1 specifically induces membrane ruffling and lamellipodia formation (Nobes and Hall, 1995; Ridley et al., 1992), while CDC42 mediates the formation of filopodia and actin micro-spikes, both necessary for directional movement of cells, CDC42 has also been reported to regulate the alignment of chromosomes during prometaphase and metaphase (Kozma et al., 1995; Yasuda et al., 2004).

Regarding the importance of these Rho GTPases in tumor cell migration and invasion, it has been reported that the p53 tumor suppressor regulates cell migration by inhibiting Rac1 GTPase activity. Other tumor suppressors had been found to regulate cell motility by

suppressing Rac1 and PI3K activities. Rac1appears to be of importance to the migratory phenotypes observed in cells with PTEN deficiency and is consider to be involved in the signaling of mammalian cells migration (Guo et al., 2003).

Pak2 activation results from the interactions of the small GTPases Rac1 and CDC42 with the PDB domain at the N-terminal regulatory domain of an inactive form of Pak2, resulting in a phosphorylation/activation of Pak2 at Serine 20. Conversely, Pak2 inhibition has been reported to be the result of the interaction and formation of Erbin and Merlin complexes binding and displacing the GTP-bound Rac1-CDC42-Pak2 complex in epithelia (Wilkes et al., 2009; *Figure 1.4*). Merlin/Erbin/Pak2 complex formation appears to be cell type dependant in that high levels of Merlin in epithelial cells are able to form the complex with increased expression of Erbin, inhibiting Pak2 activation. this is important since in fibroblasts Pak2 activation provides growth stimulatory signals (Rangwala et al., 2005; Wilkes et al., 2009).

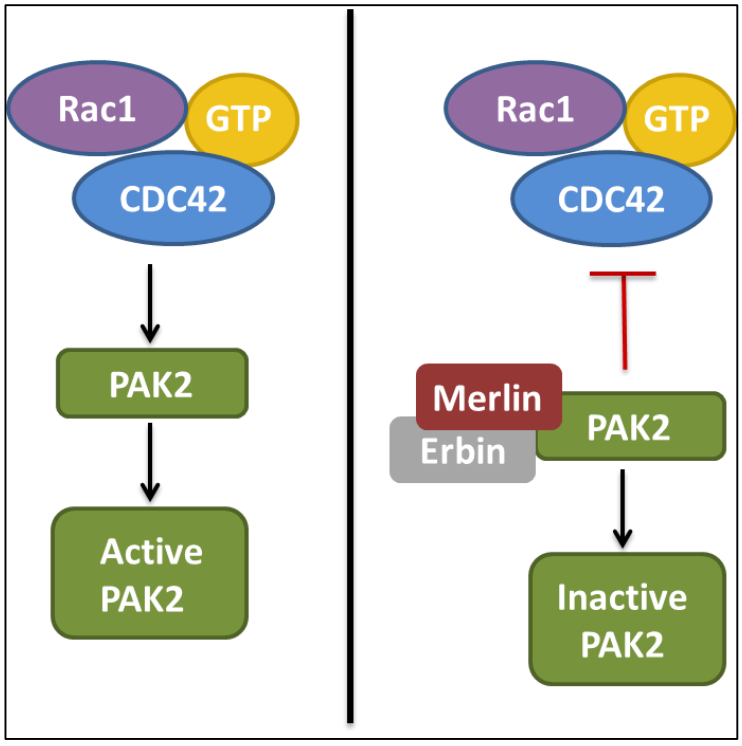

Figure 1. 4 - Pak2 activation and inhibition.

Rac1 and CDC42 interaction results in Pak2 activation (left panel). Merlin and Erbin heterodimer disrupt Pak2 interaction with Rac1 and CDC42 inhibiting its activation.

1.6.2 Pak2 Inhibitor Erbin

The LAP [leucine-rich repeat and PDZ domain (PSD-95; Dlg1; ZO-1)] family member protein Erbb2 interacting protein (Erbin) was originally reported to be a binding partner for ErbB2 subunit of the EGF receptor and was proposed to act as a mediator of basolateral trafficking (Borg et al., 2000). Since then, Erbin was characterized for its regulatory roles. Some examples include: Erbin interacts with the p120-catenin family members, Erbin has also been reported to help suppress the MAPK signaling pathway by binding to Sur-8 and disrupting the Sur-8-Ras-Raf complex (Rangwala et al., 2005), Erbin binds to Smads blocking their

oligomerization and decreasing their transcriptional output, regardless of phosphorylation status (Dai et al., 2007; Warner et al., 2003).

Erbin is ubiquitously expressed and implicated in regulating many aspects of biological behaviors of cancer cells such as cellular proliferation, apoptosis and inflammatory responses (Borg et al., 2000). There are reports demonstrating that levels of Erbin are significantly decreased or lost in cervical cancer tissues. However there has been no description of Erbin levels in prostate cancer. This loss of Erbin has been reported to provide cervical cancer with resistance to anoikis by inhibiting STAT3 signaling (Hu et al., 2013). It has also been reported that Erbin plays a positive role in ErbB2-dependent (HER2) breast tumor growth (Tao et al., 2014). The exact role that Erbin plays during tumorigenesis or the mechanism by which it is regulated is not well understood.

1.6.3 Pak2 Inhibitor Merlin

The ubiquitously expressed tumor suppressor Merlin, also known as Neurofibromatosis type 2 (NF2) or schwannomin, is part of the ERM (ezrin, radixin, and moesin) family of proteins with the function of connecting the actin cytoskeleton to various membrane-associated proteins (Golovnina et al., 2005). Merlin has been reported to interact with a number of protein partners in order to inhibit many signaling pathways. Overexpression, absence or mutations of this gene results in the generation of tumors, including schwannomas, meningiomas, and ependymomas (Bretscher et al., 2002). Interestingly, Merlin is localized to adherent junctions and physically interacts with its components, suggesting that Merlin helps control the assembly of adherent junctions and contact-dependent growth inhibition in sites of cell-cell contact. These results suggest that the loss of adherent junction function may be a mechanism by which Merlin

deficiency leads to tumor and metastasis development (Bretscher et al., 2002; Lallemand et al., 2003).

The tumor suppressor activities of NF2 are closely linked to the critical roles of Merlin in contact inhibition of cell growth and proliferation by functioning as an upstream activator of the Hippo pathway (Hamaratoglu et al., 2006), in the last two decades Merlin mutations have been identified in Neurofibromatosis type 2 and other cancer patients (Rouleau et al., 1993; Bianchi et al., 1994; Schroeder et al., 2014). Despite this, the upstream regulators of Merlin in the Hippo pathway are poorly understood and there is no current information regarding Merlin involvement in prostate cancer.

One of the other interactions reported between Merlin and Pak2, has been shown in the context of Merlin acting as a direct substrate for Pak2. The interaction of Merlin alone with Pak2 results in the phosphorylation of Merlin at the serine 518 (McClatchey and Giovannini, 2005). The phosphorylated form of Merlin has lost its ability to bind Erbin and disrupt Pak2 interaction with Rac1 and CDC42. Phosphorylation of Merlin results in its inactivation and degradation (Kissil et al., 2003; Wilkes et al., 2009; Xiao et al., 2002), suggesting Pak2 kinase activity is a mechanism by which the cell regulates Merlin function.

1.7 TGF-β interaction with Pak2 Pathway

The interaction of TGF-β ligand with its receptors TGFβRI and TGFβRII results in the activation of the PI3K pathway in a cell type specific manner. In mesenchymal cells TGF-β activation of the PI3K pathway, leads either to the activation of the AKT arm of the pathway and/or the activation of Pak2 (Wilkes et al., 2003; Wilkes et al., 2005; Moustakas and Heldin, 2005; *Figure 1.5*). Although it is not fully understood how downstream of PI3K, the pathway

recruits Rac1 and CDC42, Pak2 is activated through the interactions of Rac1 and CDC42. When Pak2 is inhibited it is due to interference by the formation of the Merlin and Erbin dimer. This dimer disrupts Pak2 interaction with Rac1 and CDC42 (Wilkes et al., 2009). Additionally, Pak2 is capable of stimulating ERK phosphorylation (Hough et al., 2012) but may also be capable of inactivating Merlin by phosphorylating it at Serine 518 (Kissil et al 2002).

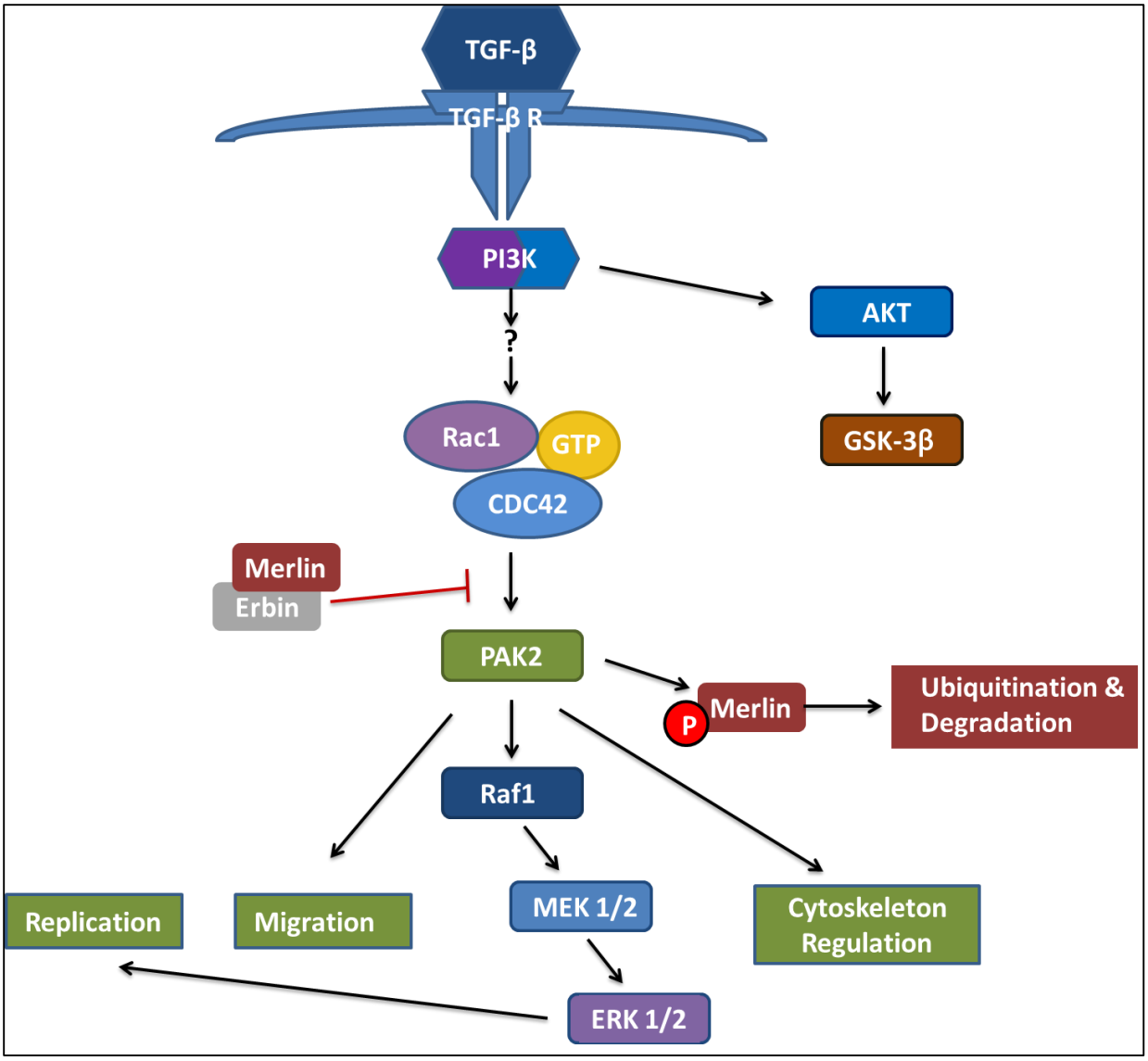

Figure 1. 5 - TGF-β promotes the activation of the Pak2 pathway

Pak2 activation is due to its interaction with Rac1 and CDC42. Merlin and Erbin disrupt Pak2 interaction with Rac1-CDC42 leading to its inactivation. Pak2 phosphorylates Merlin in the Serine 516 leading it to its degradation.

1.8 Rationale and Hypothesis

The effect, consequences or presence of active Pak2 in prostate cancer has not been fully elucidated. The steady-state expression levels of the Pak2 pathway proteins in prostate cancer are unknown although studies on mRNA levels suggest no change from normal (Siu et al., 2010). Previous findings have indicated that Pak2 is involved in the regulation of growth and migration of both normal and cancer cells, more specifically, in the promotion of invasion and migration in epithelial cancers (Goc et al., 2012; Siu et al., 2010; Somanath and Byzova, 2009; Wilkes et al., 2003, 2009). Interestingly, TGF-β has been implicated in promoting invasion and migration in later stages of prostate cancer, and has also been shown to be secreted by prostate cancers (Massagué, 2008; Moustakas and Heldin, 2007). Since prostate adenocarcinoma undergoes EMT for the development of metastasis and Pak2 mediates TGF-β stimulation in mesenchymal cells, this suggests a potential mechanism for prostate cancer alteration in the response to TGF-β (Hough et al., 2012). This thesis will address the expression levels of the Pak2 pathway components in prostate cancer cell lines, in order to address the hypothesis: ***Pak2 activation is involved in the aberrant migration of prostate cancer.***

1.9 Objectives

- Define the protein and gene expression levels within the Pak2 signaling cascade in cell line models representing disease progression (inhibitory proteins: Erbin and Merlin, stimulatory proteins Rac1 and CDC42), relative to a normal control.
- Define basal and TGF-β stimulated Pak2 activity levels.
- Assess the role of TGF-β in mediating Pak2 migratory control.

Chapter II – Materials and Methods

2.1 Cell culture

Human prostate cancer cells: 22RV-1 (CRL-2505), LNCaP (CRL-1740), PC-3 (CRL-1435), and DU145 (HTB-81) and human normal prostate epithelial cell RWPE-1 (CRL-11609) were obtained from ATTC (American Type Culture Collection; Manassas, VA). Prostate cancer cells were grown in their specified growth medium according to ATTC (*shown in Table 2.1*), supplemented with (FBS) fetal bovine serum, as described (PAA Labs Inc.; Etobicoke, ON). For drug treatment experiments prostate cancer cells were incubated for 24 hours in their respective media, supplemented with 1% FBS, while RWPE-1 cells were incubated in K-SFM media, supplemented with 0.05mg/ml of BPE. For the wound healing assay DU145 cells were seeded (8×10^4) in 24-well plates and grown to confluence for 48 hours. Growth media was supplemented with reduced serum (1% FBS) for 24 hours prior to addition of treatments to reduce effects due to replication. For other experiments cells were seeded (1×10^5) in 6-well plates and allowed to attach for 48 hours.

Table 2. 1 - – Prostate cell lines and characteristic

Cell Name	Cells Derived	Biosafety Level	Tumorigenic	Growth Medium	Added Components	Reference
RWPE-1	Epithelial cell line derived from the peripheral zone	2	No	K-SFM	0.05mg/ml PBE and 5ng/ml EGF	(Bello D et al., 1997)
22RV-1	Prostate cancer cell line derived from a Xenograft	2	Yes	RPMI-1640	10% FBS	(Sramkoski et al., 1999)
LNCaP	Lymph node metastasis	1	Yes	RPMI-1640	10% FBS	(Horoszewicz et al., 1983)
PC-3	Bone metastasis of grade IV prostate adenocarcinoma	1	Yes	F-12K (Kaighn's Modification of Ham's)	10% FBS	(Kaighn et al., 1997)
DU145	Brain metastasis	1	Yes	Eagle's Minimum Essential Medium (EMEM)	10% FBS	(Stone et al., 1978)

2.2 Western Blotting

Cells were lysed with (RIPA) Radio-Immunoprecipitation Assay Buffer (*Table 2.2)* and quantified for total protein using a BCA (Bicinchoninic acid) protein assay with a standard curve generated using BSA as reference (Pierce/ThermoFisher Scientific; Waltham, MA). Equivalent amounts of total protein were separated by polyacrylamide gel electrophoresis and then transferred into a polyvinyl difluoride (PVDF) membrane (Immobilon-P; Billerica, MA). Primary antibody binding was detected using goat anti-rabbit (Life Technologies/ThermoFisher; Carlsbad, CA), goat anti-mouse, goat anti-sheep, HRP conjugate secondary antibody as appointed in Table 2.3. (Santa Cruz Biotechnology; Santa Cruz, CA). Specific protein detection was visualized with SuperSignal West Pico Chemiluminescent Substrate (ThermoFisher; Waltham, MA) and obtaining images of the membranes on the ImageQuant LAS 4000 imager and analyzing band densities with ImageQuant TL Software (GE Healthcare Life Sciences; Mississauga, ON). Blots were stripped in a solution of 2% SDS, 63mM Tris-HCL (pH 6.8), and

0.1 M β-mercaptoethanol for 10 min at 50 °C. Stripping solution was removed by two washes of Tris-buffered saline Tween 20 [(TBST) 50mM Tris, 150mM NaCL, and 0.05% Tween 20] at room temperature, followed by blocking and incubation with α-Tubulin antibody to act as loading control.

Table 2. 2 - RIPA Buffer components and concentrations

RIPA Buffer	
Stock Solution	**Volume**
10X PBS	0.25 ml
10% Triton-X	0.25 ml
10% Deoxycholic Acid (DOC)	0.125 ml
1M TRIS-HCL pH7.4	0.125 ml
1M β-glycerophosphate	0.125 ml
1M Sodium Fluoride (NaF)	0.125 ml
0.5M Ethylenediaminetetraacetic acid (EDTA) pH7.5	25µl
20% Sodium Deodecyl Suldate (SDS)	12.5µl
10X Protease Inhibitor	0.25 ml
PMSF (Phenylmethylsulfonyl fluoride) (50µg/ml)	7.5µl
Sodium Orthovanidate (200mM)	25µl
Autoclaved dH_2O	1.18 ml
Final Volume	2.5 ml

Table 2. 3 - Western Blot antibodies, source and dilutions

Primary Antibody	Isotype	Company	Catalog	Dilution	Protein Amount
α-Tubulin	Mouse	Cell Signaling	3873	1:1000	
CDC42	Rabbit	Invitrogen	A13981	1:1000	30 µg
Cdc42 (11A11)	Rabbit	Cell Signaling	2466	1:1000	30 µg
Erbin	Sheep	R&D Systems	AF7866	1:2000	50 µg
Phospho-p44/42 MAPK (Erk1/2)	Rabbit	Cell Signaling	4377	1:1000	10 µg
P44/42 MAPK (Erk1/2)	Rabbit	Cell Signaling	9102	1:1000	10 µg
PAK2	Rabbit	Cell Signaling	2608	1:1000	30 µg
Phospho-GSK-3β (Ser9)	Rabbit	Cell Signaling	9323	1:1000	10 µg
GSK-3β	Rabbit	Cell Signaling	93150	1:1000	10 µg
Phospho-Merlin (Ser518)	Rabbit	Cell Signaling	9163	1:1000	30 µg
Phospho-Merlin (Ser518) (D5A4I)	Rabbit	Cell Signaling	13281	1:1000	30 µg
Anti-NF2 / Merlin	Rabbit	Epitomics	3357-1	1:10,000	30 µg
Rac1/2/3	Rabbit	Cell Signaling	2465	1:1000	30 µg
Rac1/Cdc42	Rabbit	Cell Signaling	4651	1:1000	30 µg

2.3 Drug Treatment

Human prostate cancer cells were incubated un reduced serum media conditions (1% vs 10%) in their respective media as described in section 2.1. The cells were treated with recombinant human transforming growth factor β1 (TGF-β; Gibco/ThermoFisher; Carlsbad, CA) at a concentration of 5ng/ml, EGF (United States Biological/Cedarlane Laboratories; Salem, MA) at a concentration of 50ng/ml, Rac1 inhibitor, RacII (EMD Millipore; Etobicoke, ON) at a concentration of 50µM, CDC42 inhibitor, ML141 (EMD Millipore; Etobicoke, ON) at a concentration of 10µM for the indicated time, and/or Pak2 inhibitor, Frax1036 (Genentech, CA) at a concentration of 1µM for the indicated time. All inhibitors were dissolved in DMSO. Doses were obtain following titration of cytotoxic effects determined experimentally by testing cells with doses of drug over 2 log orders dilutions.

2.4 RNA Extraction and cDNA Synthesis

Cells were seeded (10^6 cells/well) in a six-well plate 24 hours prior to treatment. Following treatment of Trizol reagent was added to each well (Ambion/ThermoFisher Scientific; Carlsbad, CA) for RNA extraction as per manufacture's instructions. The upper aqueous phase was collected and loaded into a Pure Link RNA Mini column (Ambion/Invitrogen; Grand Island, NY). Total RNA was isolated according to the manufacturer's instructions, with RNA integrity being assessed with the Agilent RNA 6000 Nano kit on the Bioanalyzer (Agilent Technologies; Santa Clara, CA) according to the manufacturer's instructions. Synthesis of complementary DNA (cDNA) was implemented following Applied Biosystems High-Capacity cDNA Reverse Transcription kit protocol (Applied Biosystems/ThermoFisher; Foster City, CA). In each reaction 1-2 µg of total RNA was used to synthesize cDNA. Samples were diluted with sterile H_2O to a final concentration of 10ng RNA/cDNA/µl to produce a working stock solution.

2.5 Quantitative PCR (qPCR)

qPCR was performed to measure steady state levels of Merlin, Erbin, CDC42, and Rac1 gene expression in prostate cancer cells and RWPE-1 cells (*Table 2.4*). A master mix including the TaqMan Gene Expression Master Mix 2X (Applied Biosystems/ThermoFisher; Foster City, CA), the probe of interest 20X (Applied Biosystems/ThermoFisher; Foster City, CA), 1µl of the cDNA (10ng RNA/cDNA), and nuclease-free water to have a final volume of 21µl per reaction. Samples were analyzed on ViiA™ 7 Real-Time PCR System (Applied Biosystems/ ThermoFisher; Foster City, CA) using the standard 40 cycles run in the system. Data was analyzed with the relative quantitative comparison threshold cycle (ΔΔCt) method using GAPDH as a control. GAPDH was selected from a group of control probes (18S, HPRT1, and

GUSB, and β-actin), based on its consistency between the different cell lines and linearity of detection over 3 log order dilutions.

Table 2. 4 - qPCR TaqMan Probes list

TaqMan® Probes	
GAPDH	Hs03929097_g1
CDC42	Hs00918044_g1
RAC1	Hs01025984_m1
NF2	Hs00966302_m1
ERBB2IP	Hs01049966_m1

2.6 Wound healing assay for cell migration

Prostate cancer cells were seeded at various cell number/well (DU145, 8×10^4; PC-3, 1×10^5; RWPE, 1×10^5) in 24-well plates. Wounds were made using a 200μl pipet tip in confluent cells, cultured in 24-well plates. Cells were treated with ML141 (10μM), Frax1036 (1μM), TGF-β (5μg/ml), and a combination of ML141 or Frax1036 with TGF-β, the cells were allowed to migrate into the uncovered area for 12 hours. Doubling time for DU145 is established to be at 34 hours in the its corresponding complete culture media (Webber et al., 1997), and for PC-3 doubling time is consider to be approximately 33 hours in its corresponding complete culture media (Keer et al., 1990; Rossi and Zetter, 1992). Cell migration was visualized at 10× magnification using an inverted Nikon Diaphot microscope (Nikon Instruments Inc.; Melville, NY), photographed with a Nikon digital camera D3000 at time 0 and 12h. Plates were marked with two lines perpendicular to the wound to ensure correct repeated location of the images. Cell free areas were measured as pixel units with the Image J software (National Institute of Health; Bethesda, MD).

2.7 Statistical Analysis

The difference between experimental groups was analyzed by one-way analysis of variants (ANOVA) followed by a Turkey's post hoc test. P values less than 0.05 were considered significant (*P < 0.05; **P < 0.01; ***P < 0.0005; ****P < 0.0001). Statistical analyses were performed with Prism 6 software (GraphPad Prism; La Jolla, CA). Each sample for qPCR was analyzed in triplicate from a minimum of three RNA replicates isolated from each cell line. Samples for western blotting were analyzed from a minimum of five independent protein lysates from each cell line. Migration of each cell line was analyzed using a minimum of eight replicates of each treatment.

Chapter III Results

3.1 Pak2 protein levels in Prostate Cancer

In normal mesenchymal cells the interaction of the TGF-β-receptors I and II activates the PI3K pathway, which in turn promotes the activation of the Pak2 pathway. Although prostate cancer originates from the uncontrolled growth of epithelial cells that do not activate Pak2 in response to TGF-β (Wilkes et al., 2003), we believe the EMT process alters the molecular signaling pathways to produce mesenchymal signals in epithelial cells. I therefore wanted to first examine the steady state levels of proteins within the Pak signaling cascade.

In order to observe the expression levels of Pak2 protein in prostate cancer, immunoblots were performed with a panel of four different prostate cancer cell lines to model different stages of prostate cancer progression (*Figure 3.1*). These levels were compared to a non-malignant control RWPE-1. α-Tubulin expression was used as a loading control. The cell lines used were: 22Rv1 (primary tumor), LNCaP (early androgen responsive tumor), PC-3 and DU145 (androgen independent, late tumor), and the normal prostate epithelial cell RWPE (immortalized but non-tumorigenic). Pak2 protein levels show variation between the prostate cancer cell lines. The early tumor cell line LNCaP and the late tumor cell line DU145 show a statistically significance difference from the non-malignant control RWPE-1 cell line. However, despite these differences there appears to be a significant amount of Pak2 protein in the cell lines with reduced expression.

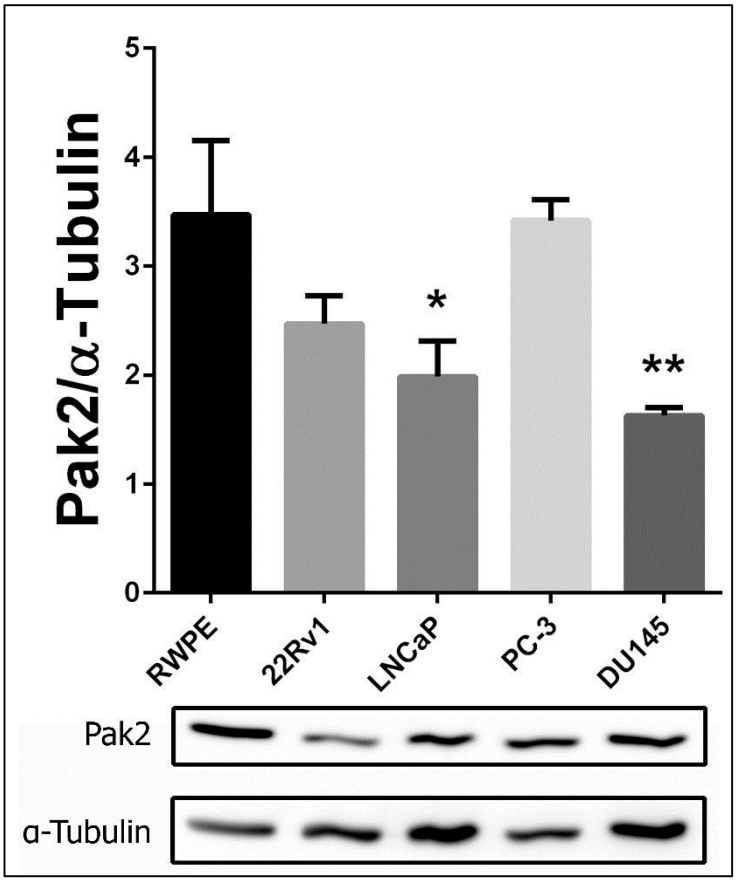

Figure 3. 1 - Pak2 protein expression levels

Protein expression levels of Pak2 in prostate cancer cell lines corrected for loading control using α-Tubulin, were determined. Immunoblots (n=5) from five separate cell lysate were performed and ANOVA statistical analysis was performed (*P<0.05; **P<0.01). Units shown on the y-axis represent pixel density for Pak2 immunoblots derived over the pixel density for α-Tubulin for the same blot.

3.2 Pak2 stimulatory proteins (Rac1 and CDC42)

Pak2 activation is due to its interactions with the GTPase proteins Rac1 and CDC42 (Lei et al., 2000). In order to determine the levels of the Pak2 stimulatory proteins Rac1 and CDC42, immunoblots were performed with an antibody capable of detecting total amount of both proteins in the total cell lysates from prostate cancer cell lines 22RV-1, LNCaP, PC-3, and

DU145 compared to the non-malignant control RWPE. α-Tubulin antibody was used as a loading control. Analysis of the immunoblots showed a significant difference of total amount of Rac1 and CDC42 protein levels (*Figure 3.2*) in all prostate cancer cell lines, especially in the later stage tumor cell line DU145, compared to the non-malignant control RWPE.

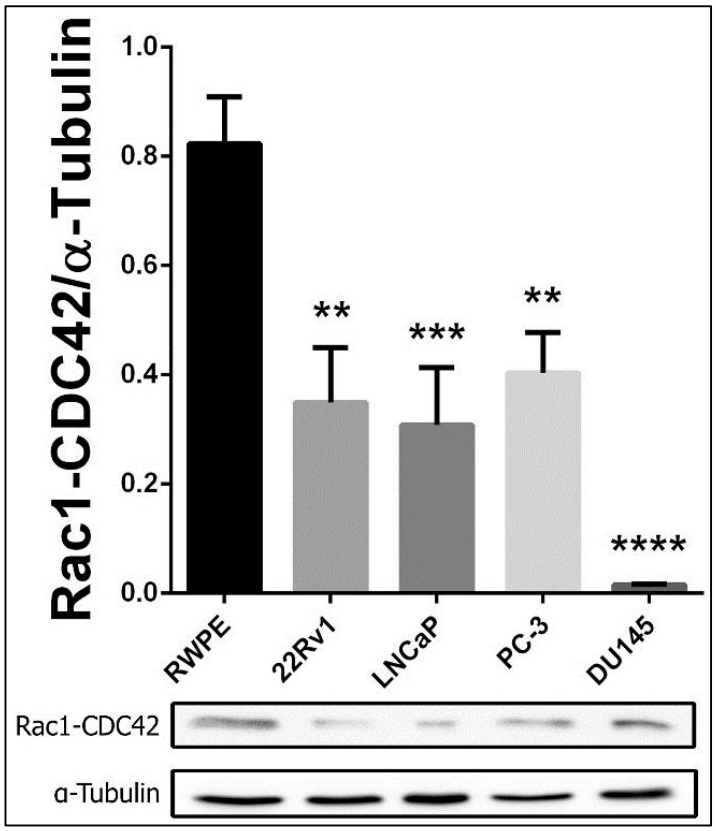

Figure 3. 2 - Total protein levels of the Pak2 stimulatory proteins Rac1 and CDC42

Steady state expression levels of the Pak2 stimulatory proteins Rac1 and CDC42. Immunoblots (n=5) were used to identify both proteins, using α-Tubulin as a loading control. Pixel densities from each immunoblot were analyzed relative to RWPE (ANOVA and Tukey's post hoc) to determine significance (*P<0.05; **P<0.01; ***P < 0.0005; ****P < 0.0001).

3.3 Rac protein and RNA expression levels

Similar to what was observed when total expression of total Rac1 and CDC42 was determined, when we analyzed prostate cancer cell lysate for total Rac (Rac1, 2, 3; *Figure 3.3A*). A significant reduction of total Rac was found in all cell lines, with a trend to lower levels with advancement of disease (22RV-1 vs PC-3 – P = 0.058, 22RV-2 vs DU145 – P = 0.0021).

Of all the Rac isoforms (Rac1, 2, or 3) Rac1 is the most abundant of all three Rac proteins (Nobes and Hall, 1995). This data suggests that Rac1 protein levels decrease with advancement of the disease. In order to determine if the protein levels are the result of decreased gene expression of Rac1, a qPCR was performed on steady state mRNA expression levels of Rac1 (*Figure 3.3B*). Interestingly, Rac1 mRNA levels significantly increased with disease progression (LNCaP and PC-3), but Rac1 mRNA levels was not consistent and elevated in DU145, where expression was similar to the control RWPE-1.

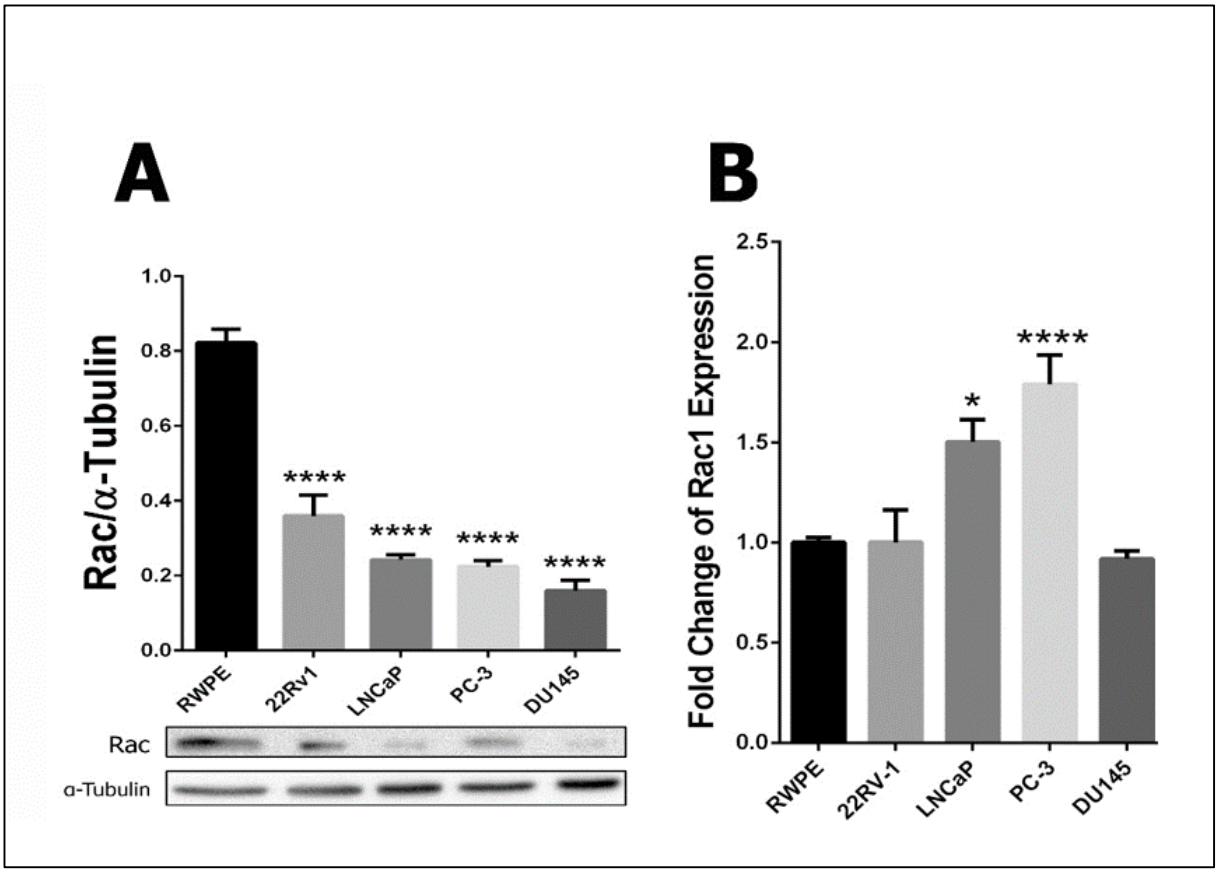

Figure 3. 3 – Total Rac protein levels and gene expression changes in prostate cancer cells

A- Steady state expression levels of the Pak2 stimulatory protein Rac1. Immunoblots (n=6) were used to determine Rac1 levels, using α-Tubulin as a loading control. Pixel densities from each immunoblot were analyzed (ANOVA and Tukey's post hoc) to determine significance (*P<0.05; **P<0.01; ***P < 0.0005; ****P < 0.0001). B- Steady state of mRNA expression levels of Rac1 was determined by qPCR (n=3). Analysis by relative quantitative threshold cycles (ΔΔCT) method was performed, results were normalized to a GAPDH internal standard.

3.4 CDC42 protein levels and RNA expression levels

Unlike Rac1, specific antibodies were available to determine the steady state levels of CDC42 (*Figure 3.4 A*). In contrast to what was observed in figures 3.2 and 3.3, relative levels of CDC42 increase corresponding to advancement of disease and the acquisition of androgen independence (PC-3 and DU145). Although the amount of CDC42 is increasing, the total levels of Rac1/CDC42 are significantly decreasing in prostate cancer cell lines compared to the control (*Figure 3.2*). Indicating the ratio of CDC42:Rac1 in these cells is changing dramatically in favor of CDC42 over Rac1.

In contrast to the protein levels, the mRNA levels of CDC42 in DU145 were lower (*Figure 3.4 B*). No significant difference in CDC42 levels were seen in most cancer cell lines relative to RWPE-1 control, with PC-3 being the exception with a 3-fold increase in CDC42 mRNA levels.

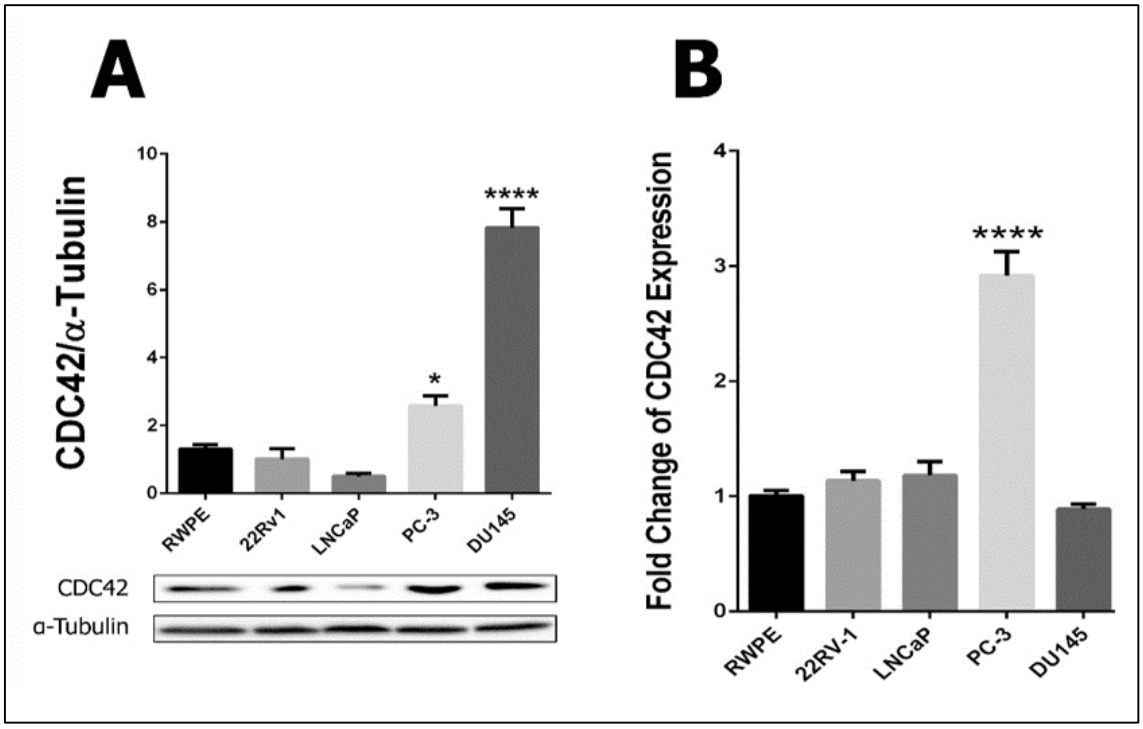

Figure 3. 4 - Total CDC42 protein levels and gene expression changes in prostate cancer cells

A- Steady state expression levels of the Pak2 stimulatory protein CDC42. Immunoblots (n=6) were used to identify CDC42, using α-Tubulin as a loading control. Pixel densities from each immunoblot were analyzed (ANOVA and Tukey's post hoc) to determine significance (*P<0.05; **P<0.01; ***P < 0.0005; ****P < 0.0001). B- Steady state of mRNA expression levels of CDC42 was determined by qPCR (n=3). Analysis by relative quantitative threshold cycles (ΔΔCT) method was performed, results were normalized to a GAPDH internal standard.

3.5 Expression levels of Pak2 inhibitor Erbin

Based on the results showing a small decrease in Pak2 protein levels and shift in ratio of the Pak2 activator proteins, I decided to examine the levels of the Pak2 inhibitory protein Erbin. In order to measure the protein expression levels of Erbin, immunoblots were performed to compare total Erbin protein expression levels on prostate cancer cell lines relative to that of RWPE control. Using α-Tubulin as a loading control. Analysis of the protein levels demonstrate

a significant reduction on Erbin protein levels in all prostate cancer cell lines compare to RWPE. qPCR and analysis of mRNA levels were performed to measure Erbin mRNA expression. Opposite to what the Erbin protein levels showed (*Figure 3.5 A*), the change of Erbin gene expression in the prostate cancer cell lines LNCaP and DU145 show a significant increase of 3 and 8-fold respectively (*Figure 3.5 B*) in comparison to the control RPWE with no difference seen in 22RV-1 or PC-3.

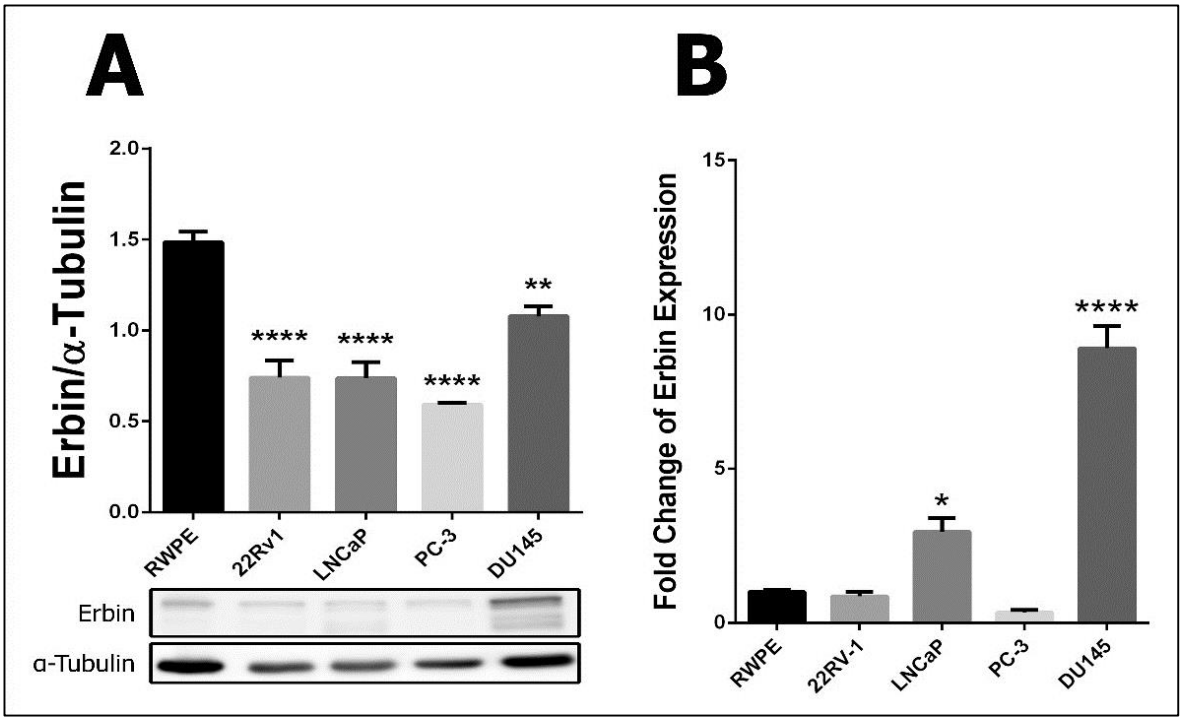

Figure 3. 5 - Total protein levels of the Pak2 inhibitory protein Erbin and gene expression levels

A- Steady state expression levels of the Pak2 inhibitory protein Erbin. Immunoblots (n=6) were used to identify Erbin, using α-Tubulin as a loading control. Pixel densities from each immunoblot were analyzed (ANOVA and Tukey's post hoc) to determine significance (*P<0.05; **P<0.01; ****P < 0.0001). B- Steady state of mRNA expression levels of Erbin was determined by qPCR (n=3). Analysis by relative quantitative threshold cycles (ΔΔCT) method was performed, results were normalized to a GAPDH internal standard.

3.6 Expression of levels of Pak2 inhibitor Merlin

Based on the observation of previous results showing a shift in the ratio of the Pak2 activator proteins from Rac1 to CDC42 (*Figure 3.3 vs 3.4 in context of figure 3.2*), the small decrease in Pak2 protein and the decrease in the inhibitory protein Erbin, the levels of Merlin, the other Pak2 inhibitory protein, were examined. Total Merlin protein expression was measured by immunoblots on prostate cancer cell lines and compared to the control RWPE. Analysis of protein data indicate significantly higher Merlin protein levels in all prostate cancer cells compared to RWPE (*Figure 3.6 A*). qPCR for Merlin gene expression levels was assessed using GAPDH as an internal standard. The change in Merlin gene expression in the prostate cancer cell lines 22RV-1, LNCaP and PC-3 show a significant increase of 2-fold, 7-fold, and 9-fold respectively (*Figure 3.6* B) in comparison to the control RPWE.

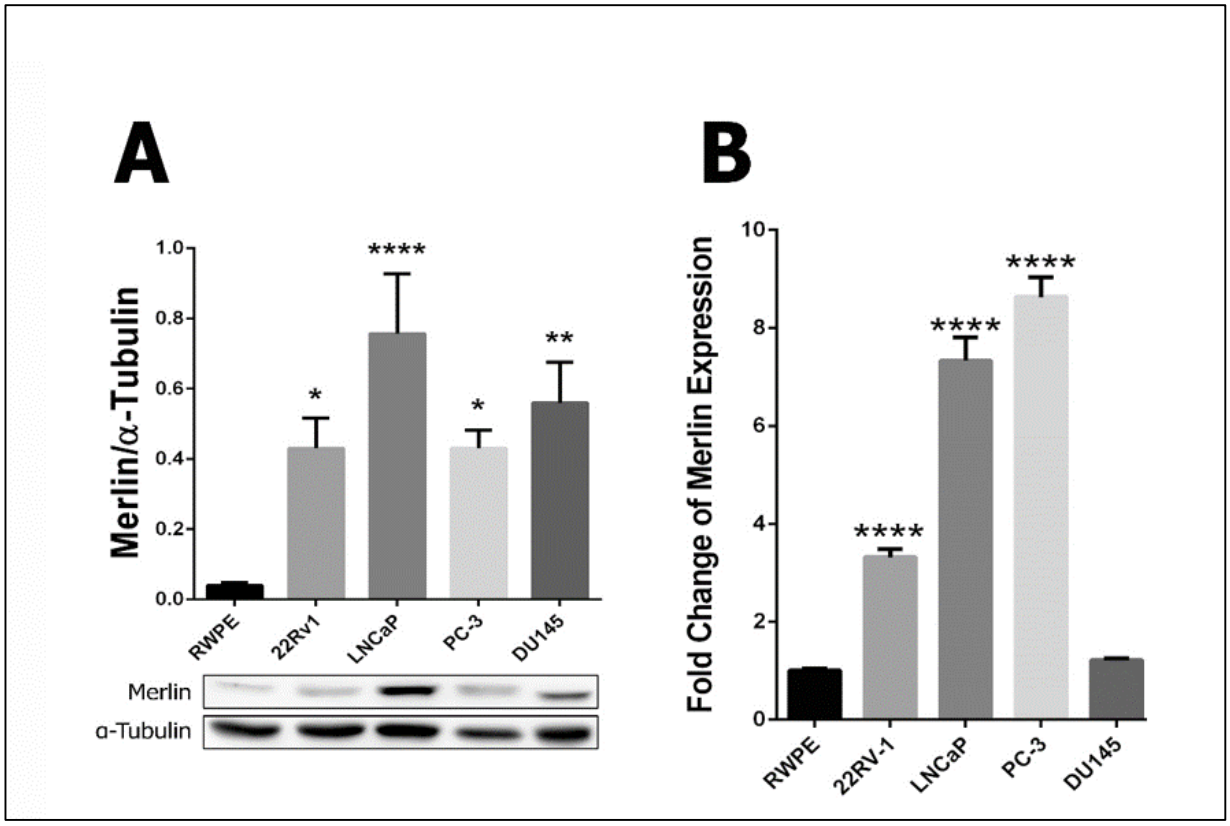

Figure 3. 6 - Total protein levels of the Pak2 inhibitory protein Merlin and gene expression levels

A- Steady state expression levels of the Pak2 inhibitory protein Merlin. Immunoblots (n=6) were used to identify Merlin, using α-Tubulin as a loading control. Pixel densities from each immunoblot were analyzed (ANOVA and Tukey's post hoc) to determine significance (*P<0.05; **P<0.01; ****P < 0.0001). B- Steady state of mRNA expression levels of Merlin was determined by qPCR (n=3). Analysis by relative quantitative threshold cycles (ΔΔCT) method was performed, results were normalized to a GAPDH internal standard.

3.7 Pak2 activity measured by Phospho-Merlin (P-Merlin) levels

Although Pak2 protein levels showed a small reduction; to observe Pak2 activity, Merlin phosphorylation was determined. Pak2 phosphorylates Merlin Serine 518 in order to impair Merlin's function. This phosphorylation directs Merlin to degradation (Kissil et al., 2002).

Immunoblots were performed in order to observe steady state Pak2 activity by means of Merlin phosphorylation. P-Merlin levels were assessed in the prostate cancer cell lines and compared to the non-malignant control RWPE-1 (*Figure 3.7 A*). The level of Pak2 activity (P-Merlin) as a function of the amount of Merlin present showed an increase in Pak2 activity in the advance prostate cancer cell lines PC-3 and DU145. However, since Merlin levels changed with disease progression (*Figure 3.6*), we wished to correct for this. Thus by analyzing P-Merlin relative to the amount of Merlin present as a function of total cellular protein (corrected for α-Tubulin), it is possible to determine relative steady state Pak2 activity. P-Merlin levels were compared against total amount of Merlin present and normalised against the loading control α-Tubulin (*Figure 3.7 B*). Analysis of the protein data indicated a significant reduction on P-Merlin levels on the 22RV-1 and LNCaP prostate cancer cell lines compared to RWPE-1 control, and a significant increase on P-Merlin levels on the PC-3 and DU145 cells in comparison to the RWPE-1 control, suggesting an increase in Pak2 activity.

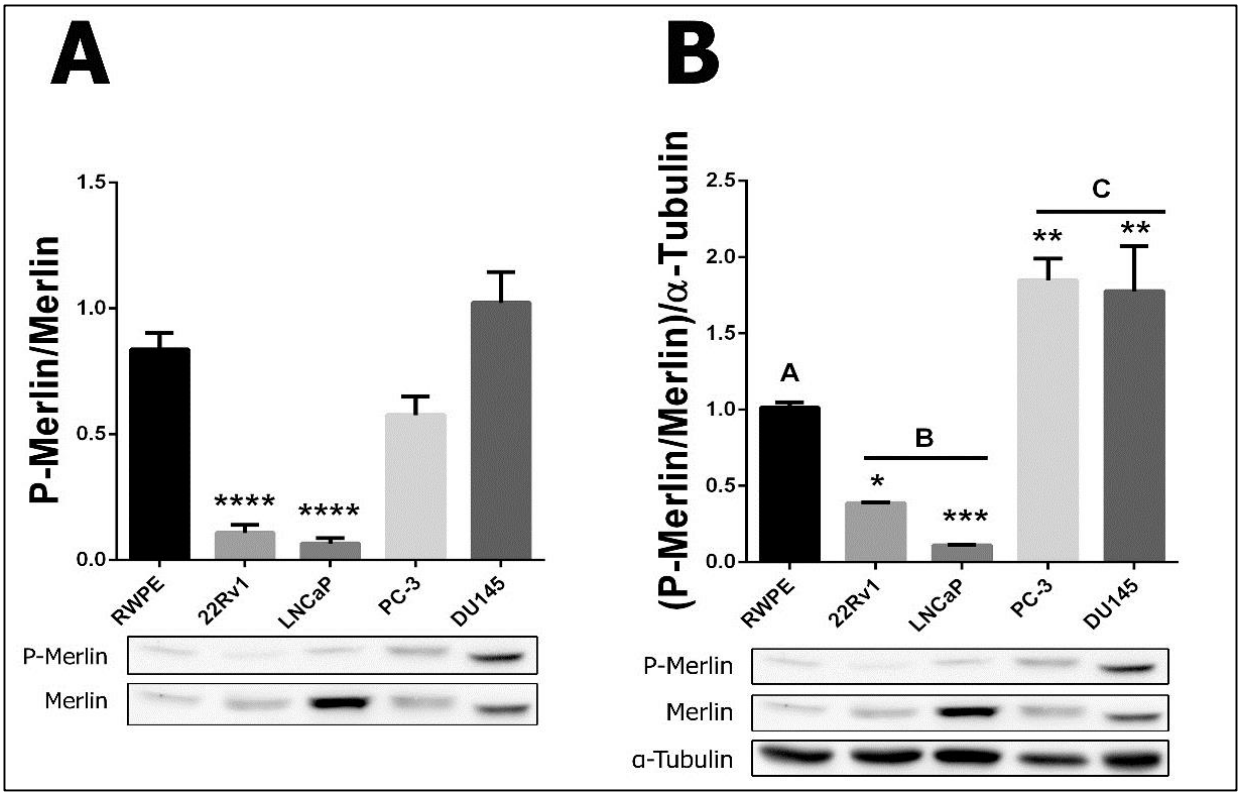

Figure 3. 7 – Pak2 activity measured by P-Merlin expression levels

A- Steady state expression levels of P-Merlin. Immunoblots (n=6) were used to identify P-Merlin, using Merlin as control. B- P-Merlin compared to total Merlin were normalized with α-Tubulin loading control. Pixel densities from each immunoblot were analyzed (ANOVA and Tukey's post hoc) to determine significance (*P<0.05; **P<0.01; ***P < 0.0005; ****P < 0.0001).

3.8 TGF-β effect on GSK-3β activity

TGF-β interaction with its receptors results in the activation of the PI3K pathway. In mesenchymal cells this activation can lead to AKT activation, therefore to the activation of GSK-3β (Grimes and Jope, 2001). Immunoblots were performed in order to assess the responsiveness of the PI3K pathway to TGF-β stimulation (Guo et al., 2008) by means of

Phospho-GSK-3β (P-GSK-3β) levels against relative amount of total GSK-3β. Treatments with TGF-β (5ng/ml) were added to the cells for two different time points (0 hours, 1 hours, and 3 hours). Levels of P-GSK-3β were corrected using total GSK-3β in order to assess the effect of the TGF-β treatment in 22RV-1 and PC-3 cell lines (*Figure 3.8*). The difference between the mean values were obtained from 6 experiments for each cell line at each time point. Analysis of the phosphorylation status of GSK-3β indicated no differences on the levels of P-GSK-3β from time 0h (unstimulated) in 22RV-1 and PC-3 cell lines with the TGF-β treatment (3h). LNCaP cells were not used in this experiment, due to the fact that LNCaP cells do not poses TGF-β receptors (Horoszewicz et al., 1983; Kim et al., 1996). Also, RWPE-1 control was not used because epithelial cells does not activate the PI3K pathway (Bakin et al., 2000; Wilkes et al., 2005). These results suggest that TGF-β is not stimulating the activation of AKT pathway as shown in figure 1.5.

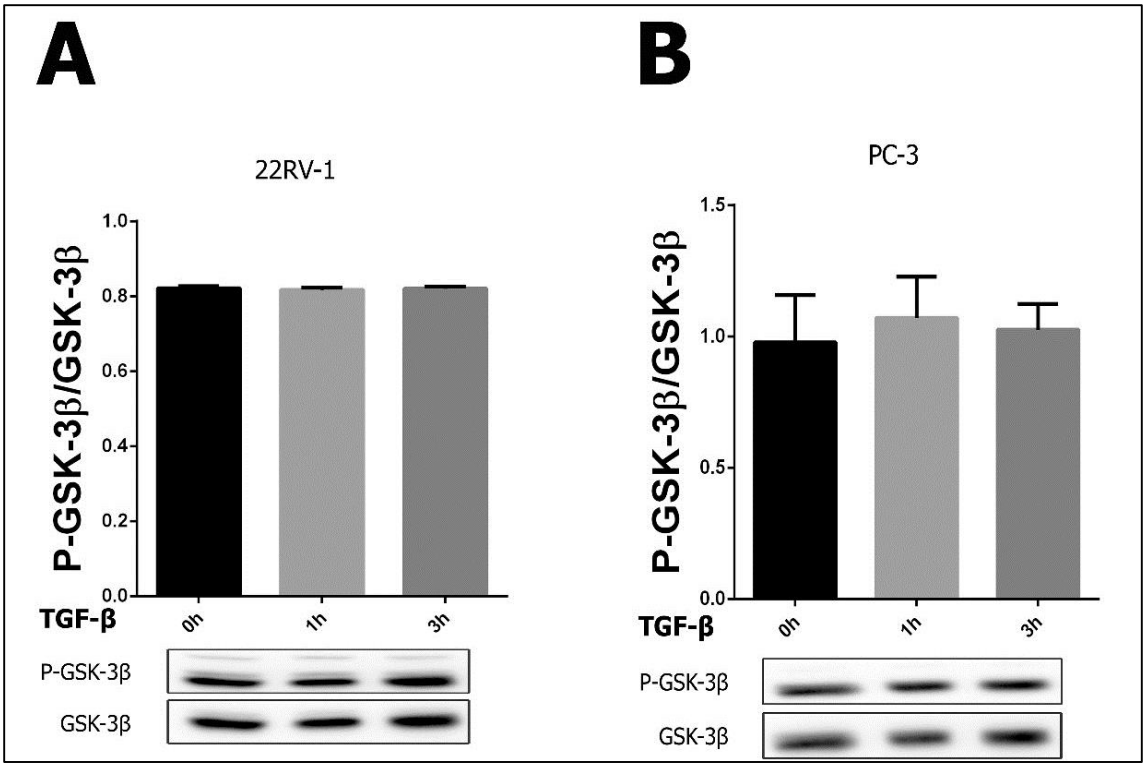

Figure 3. 8 - P-GSK-3β expression levels in the presence of TGF-β

A- Expression levels of P- GSK-3β in 22RV-1 cells with TGF-β treatment. Immunoblots (n=6) were used to identify P-GSK-3β, using total GSK-3β as control. B- Expression levels of P- GSK-3β in PC-3 cells with TGF-β treatment. Immunoblots (n=6) were used to identify P-GSK-3β, using total GSK-3β as control. Pixel densities from each immunoblot were analyzed (ANOVA and Tukey's post hoc) to determine significance (*P<0.05; **P<0.01; ***P < 0.0005; ****P < 0.0001).

3.9 TGF-β promotes ERK activation through the PI3K pathway

As observed in previous results TGF-β does not promote the activation of AKT (phosphorylation of GSK-3β) in early (22RV-1) and late (PC-3) prostate cancer cell lines. However, TGF- β promotes cell growth in mesenchymal cells (Heldin et al., 2009; Principe et al., 2014) through ERK phosphorylation via Pak2 in mesenchymal cells, but not epithelial cells (Hough et al., 2012; Wilkes et al., 2005).

Immunoblots were performed in order to review the responsiveness of this arm of the PI3K pathway to TGF-β by Phospho-ERK (P-ERK) levels against total amount of ERK (Hough et al., 2012). A treatment of 5ng/ml of TGF-β was delivered to the cells for three different time points (0 hours, 1 hours, and 3 hours). Levels of P-ERK were corrected for total amount of ERK in each cell line (*Figure 3.9*). Mean values were calculated from 6 experiments for each cell line. 22RV-1 and DU145 cells show a significant increase of 2-fold in P-ERK levels at 3 hours of TGF-β treatment in comparison to the untreated cells. Again, LNCaP cells were not used in this experiment, because LNCaP cells do not possess TGF-β receptors (Horoszewicz et al., 1983; Kim et al., 1996). PC-3 and RWPE-1 cells showed no response to TGF-β resulting in no phosphorylation of ERK (*Appendix A1*).

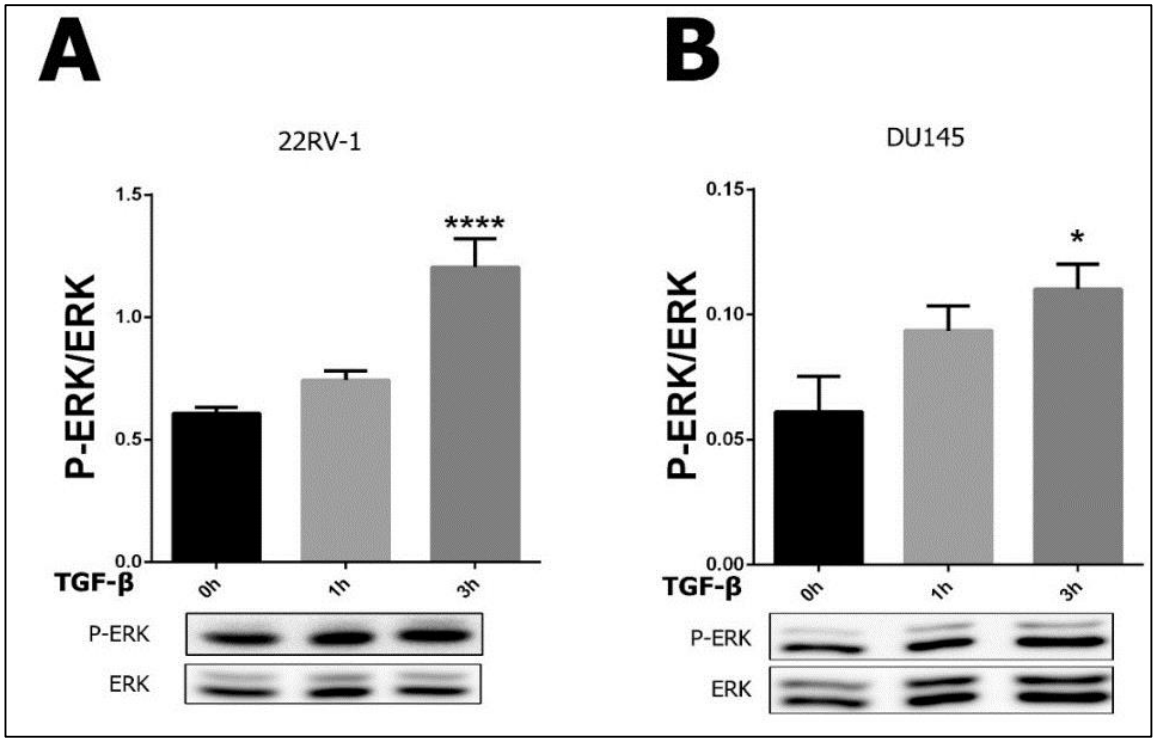

Figure 3. 9 - P-ERK expression levels in the presence of TGF-β

A- Expression levels of P- ERK in 22RV-1 cells with TGF-β treatment. Immunoblots (n=6) were used to identify P-ERK, using total ERK as control. B- Expression levels of P-ERK in DU145 cells with TGF-β treatment. Immunoblots (n=6) were used to identify P-ERK, using total ERK as control. Pixel densities from each immunoblot were analyzed (ANOVA and Tukey's post hoc) to determine significance (*P<0.05; ****P < 0.0001).

3.10 TGF-β effect on Merlin phosphorylation in prostate cell lines

3.10.1 RWPE-1 Cell Line

Previous results show that steady state Merlin phosphorylation levels increased in advanced prostate cancer cell lines and that TGF-β promotes ERK phosphorylation, indicating the possibility of the ability of TGF-β to promote Pak2 activity in prostate cancer cell lines. Merlin has also been reported to act as a direct substrate for Pak2, becoming phosphorylated at

the serine 518. This phosphorylation impairs Merlin function and leads Merlin to its degradation (Kissil et al., 2002; Wilkes et al., 2009; Xiao et al., 2002).

TGF-β influence on Pak2 activity was assessed using P-Merlin levels against the total levels of Merlin with immunoblots. Treatment with TGF-β (5ng/ml) was administrated to RWPE-1 cells for different time points (0 hours, 1 hours, and 3 hours; *Figure 3.10 A*). Levels of P-Merlin were compared against total amount of Merlin with the TGF-β treatments and normalised against the loading control α-Tubulin (*Figure 3.10 B*). As expected, normal epithelial cells do not activate Pak2 as response to TGF-β, RWPE-1 cells showed no response to TGF-β treatment, showing no difference in P-Merlin levels compared to total amount of Merlin.

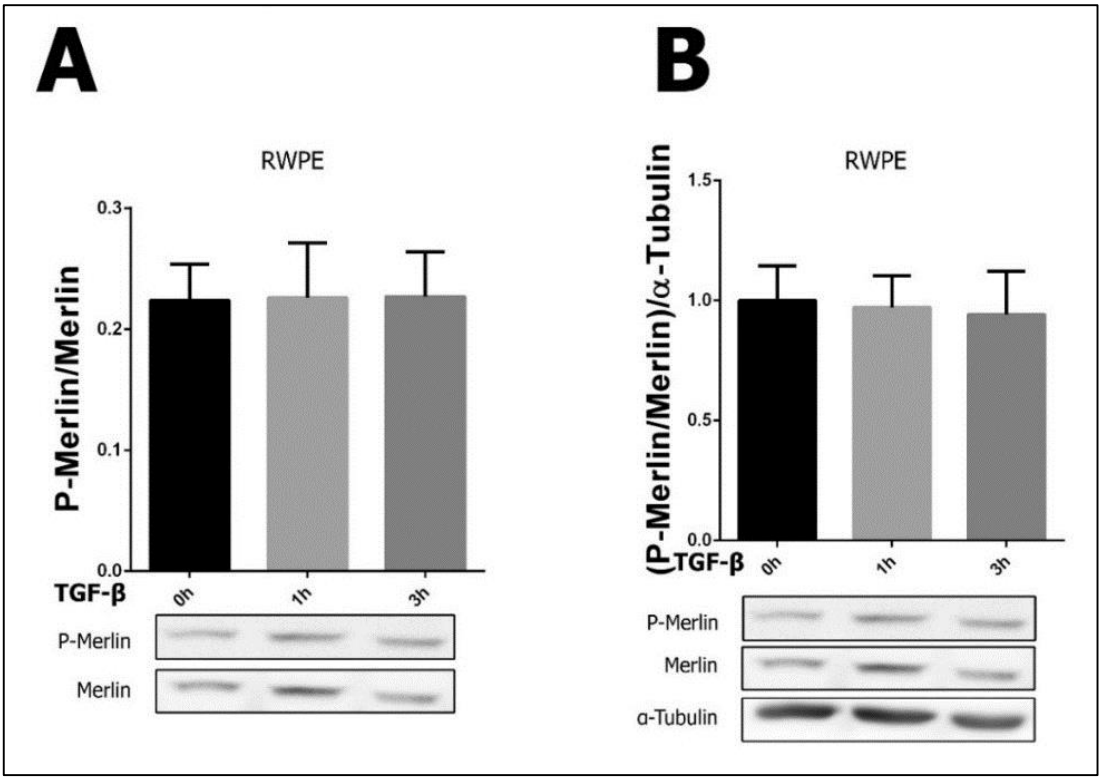

Figure 3. 10 - P-Merlin expression levels on normal epithelial cells in the presence of TGF-β

A- Expression levels of P- Merlin in RWPE-1 cells with TGF-β treatment. Immunoblots (n=6) were used to identify P-Merlin, using total Merlin as control. B- P-Merlin compared to total Merlin were normalized with α-Tubulin loading control. Pixel densities from each immunoblot were analyzed (ANOVA and Tukey's post hoc) to determine significance (*P<0.05; ****P < 0.0001).

3.10.2 22RV-1 Cell Line

The influence of TGF-β on Pak2 activity was assessed using P-Merlin levels against total amount of Merlin with immunoblots. TGF-β (5ng/ml) was administrated to 22RV-1 cells for different time points (0 hours, 1 hours, and 3 hours; *Figure 3.11 A*). Levels of P-Merlin were compared against total amount of Merlin with the TGF-β treatments and normalised against the loading control α-Tubulin (*Figure 3.11 B*). Analysis of 22RV-1 protein lysate showed a

significant increase on P-Merlin levels after 3 hours of TGF-β treatment compared to unstimulated cells (Time 0 hours).

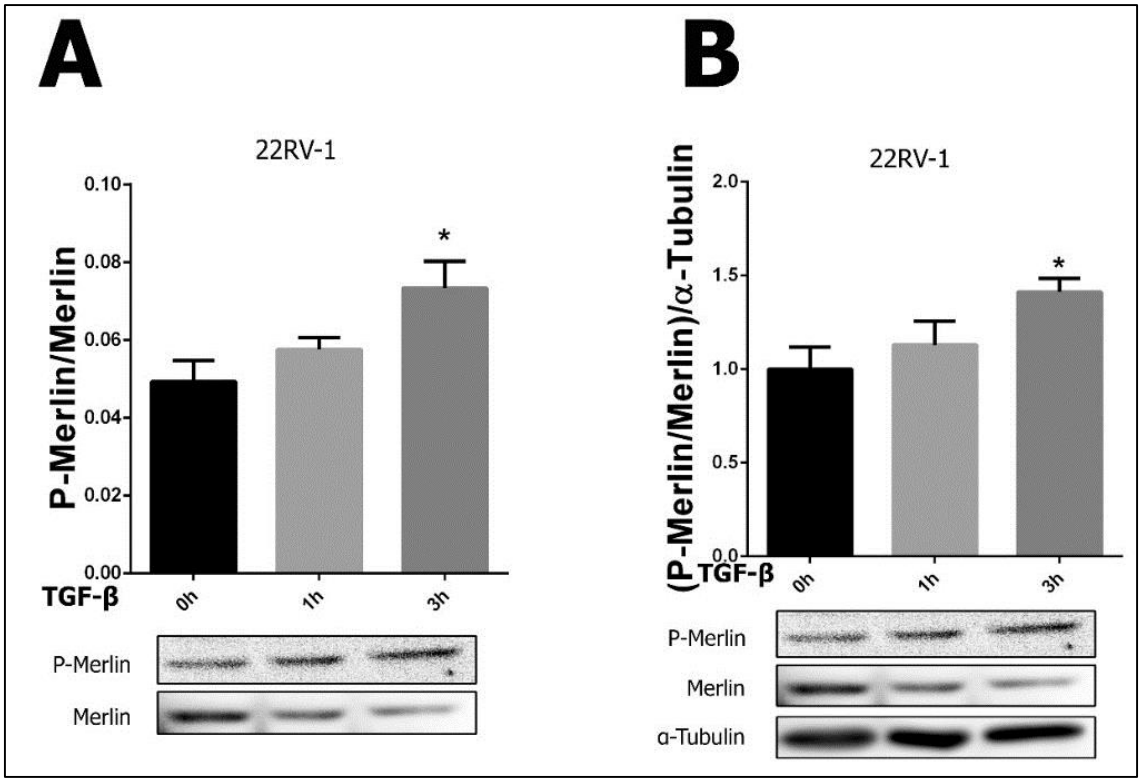

Figure 3. 11 - P-Merlin expression levels on 22RV-1 cells in the presence of TGF-β

A- Expression levels of P- Merlin in 22RV-1 cells with TGF-β treatment. Immunoblots (n=6) were used to identify P-Merlin, using total Merlin as control. B- P-Merlin compared to total Merlin were normalized with α-Tubulin loading control. Pixel densities from each immunoblot were analyzed (ANOVA and Tukey's post hoc) to determine significance (*P<0.05).

3.10.3 PC-3 Cell Line

The influence of TGF-β on Pak2 activity was determined with P-Merlin levels against total amount of Merlin present in immunoblots. Treatment with TGF-β (5ng/ml) was administered to PC-3 cell line for different time points (0 hours, 1 hours, and 3 hours; *Figure 3.12 A*). Levels of P-Merlin were compared against total amount of Merlin between the TGF-β

treatments and normalised against the loading control α-Tubulin (*Figure 3.12 B*). PC-3 cells showed a significant increase on P-Merlin levels in comparison to total amount of Merlin at 3 hours of TGF-β treatment compared to unstimulated cells (Time 0 hours).

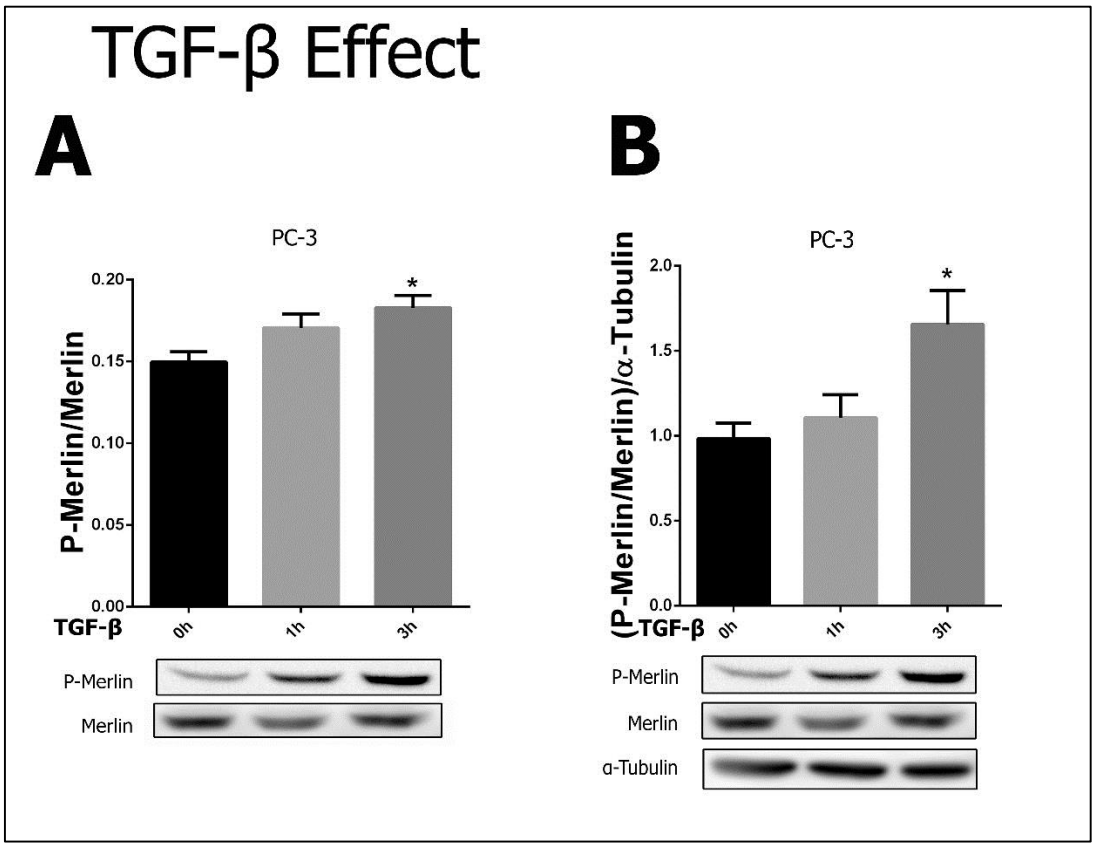

Figure 3. 12 - P-Merlin expression levels on PC-3 cells in the presence of TGF-β

A- Expression levels of P- Merlin in PC-3 cells with TGF-β treatment. Immunoblots (n=6) were used to identify P-Merlin, using total Merlin as control. B- P-Merlin compared to total Merlin were normalized with α-Tubulin loading control. Pixel densities from each immunoblot were analyzed (ANOVA and Tukey's post hoc) to determine significance (*P<0.05).

3.10.4 DU145 Cell Line

As in the other prostate cancer cell lines the influence of TGF-β on Pak2 activity was assessed with P-Merlin levels against total amount of Merlin present in immunoblots. Treatment

with TGF-β (5ng/ml) was administered to DU145 cells for different time points (0 hours, 1 hours, and 3 hours *Figure 3.13 A*). Levels of P-Merlin were compared against total amount of Merlin between the TGF-β treatments and normalised against the loading control α-Tubulin (*Figure 3.13 B*). DU145 cells showed a significant increase on P-Merlin levels in comparison to total amount of Merlin at 3 hours of TGF-β treatment compared to unstimulated cells (Time 0 hours).

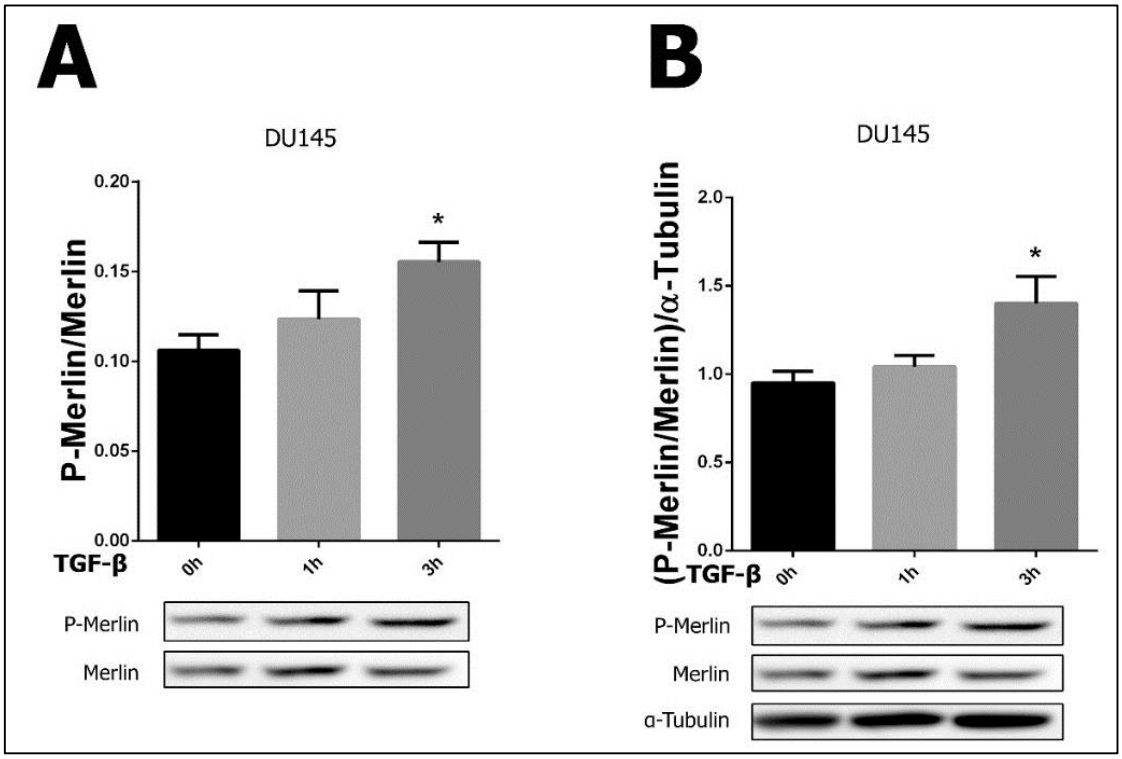

Figure 3. 13 - P-Merlin expression levels on DU145 cells in the presence of TGF-β

A- Expression levels of P- Merlin in DU145 cells with TGF-β treatment. Immunoblots (n=6) were used to identify P-Merlin, using total Merlin as control. B- P-Merlin compared to total Merlin were normalized with α-Tubulin loading control. Pixel densities from each immunoblot were analyzed (ANOVA and Tukey's post hoc) to determine significance (*P<0.05).

3.11 Effect of inhibition of the Pak2 stimulator proteins Rac1 and CDC42 on TGF-β response in prostate cell lines

Although, TGF-β does not stimulate Pak2 phosphorylation of Merlin in normal prostate epithelial cells (*Figure 3.10*), TGF-β and Pak2 each have important functions. As stated in the hypothesis (Section 1.8) I am interested in understanding how TGF-β affects prostate cancer progression and aggressiveness. As observed in previous results (*Figure 3.9*), TGF-β can aberrantly activate ERK in some prostate cancer cells and not in normal prostate epithelial cells (*Appendix A1*), while TGF-β promotes Merlin phosphorylation in all prostate cancer cell lines (Section 3.10), suggesting activation of Pak2.

3.11.1 RWPE-1 Cell Line

The effectiveness of inhibitors against the Pak2 activators Rac1 and CDC42 was assessed by immunoblots. Pak2 activity was implied by the levels of P-Merlin were compared against total amount of Merlin normalised against the loading control α-Tubulin, the effect of Rac1 inhibitors (RacII) and CDC42 inhibitor (ML141) ±TGF-β (5ng/ml) was measured (*Figure 3.14*). RWPE-1 cells treated with RacII for 6 hours and a combination of RacII with TGF-β, and ML141 with TGF-β showed a significant reduction on P-Merlin levels in comparison to total amount of Merlin in untreated cells, suggesting in normal cells steady state levels of P-Merlin are maintained primarily by Rac1. The unexpected TGF-β + ML141 (inhibition of CDC42) decreased P-Merlin ratio is difficult to mechanically explain since other experiment done in the laboratory have shown TGF-β inhibits the activation of Pak2 in other normal epithelial cell lines and may reflect alterations due to reduce serum conditions.

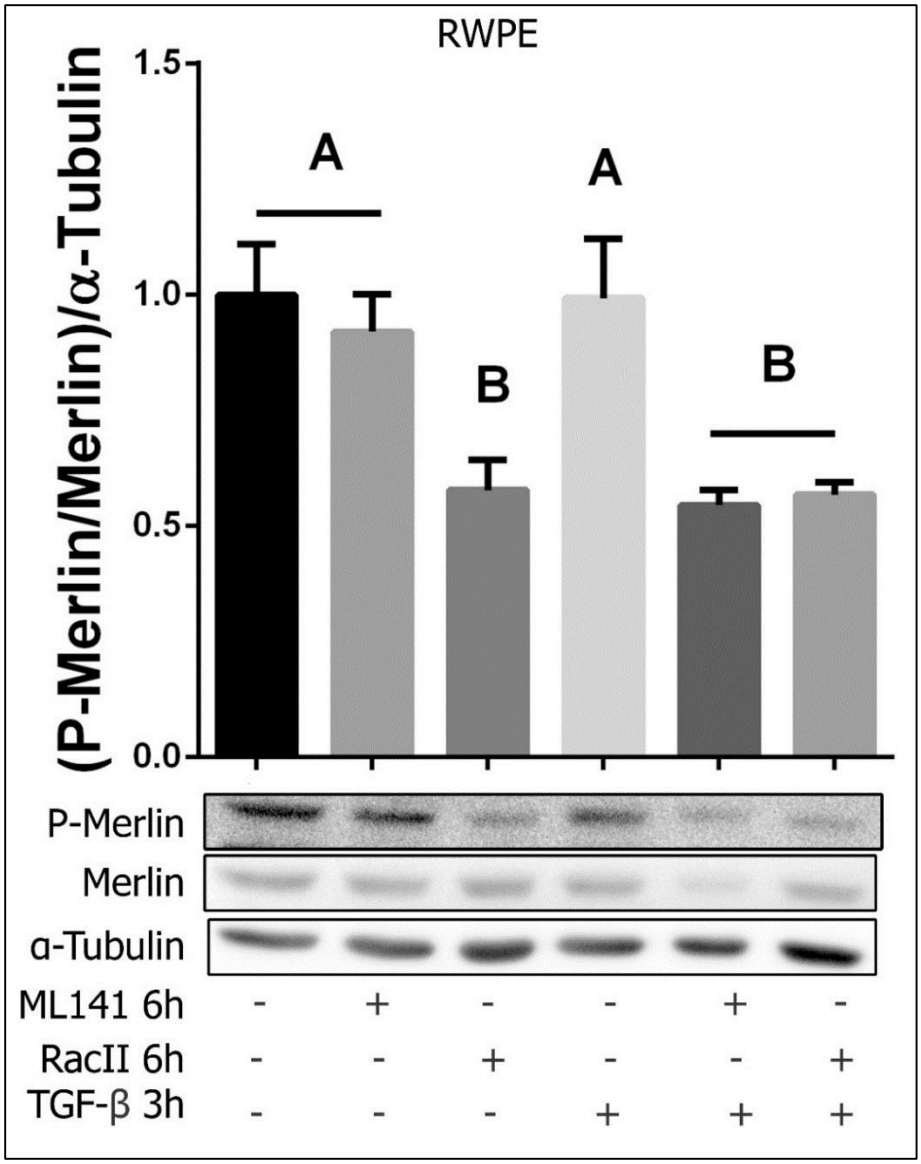

Figure 3. 14 - TGF-β effect on the inhibition of Pak2 stimulatory proteins Rac1 and CDC42 in normal epithelial cell RWPE-1

Expression levels of P-Merlin compared to total Merlin were normalized with α-Tubulin loading control in RWPE-1 cells. Immunoblots (n=6) were used to determine P-Merlin levels with ± inhibitors (ML141 & RacII) and stimulated with ± TGF-β. Pixel densities from each immunoblot were analyzed (ANOVA and Tukey's post hoc) to determine significance. Letter designations is to differentiate between different statistical groups.

3.11.2 PC-3 Cell Line

TGF-β stimulated Pak activation in prostate cell lines (*Figure 3.11- 3.13*), the effectiveness of inhibitors against the Pak2 activators, Rac1 and CDC42, was assessed by immunoblots. Stimulation of Pak2 activity was implied by the levels of P-Merlin compared against total amount of Merlin normalised to α-Tubulin. The effect of Rac1 inhibitors (RacII) and CDC42 inhibitor (ML141) in the presence or absence of TGF-β (5ng/ml) was measured (*Figure 3.15*). PC-3 cells treated with ML141 for 6 hours, with or without TGF-β (3h), showed a significant reduction in P-Merlin levels in comparison to untreated cells. As showed previously (*Figure3.12*) PC-3 cells treated with TGF-β for 3 hours showed a significant increase on P-Merlin levels. Interestingly, although there was no significant effect of the Rac1 inhibitor on P-Merlin levels relative to untreated cells, the inhibitor was able to eliminate the stimulation effect of TGF-β, restoring the P-Merlin levels to those seen with the inhibitor alone. In comparison to the control RWPE cell line (*Figure 3.14*) which I have previously shown the CDC42/Rac1 ratio to be different form PC-3 cells (showed more CDC42 than Rac1), this data is consistent with this cell-line Pak2 being primarily regulated by CDC42.

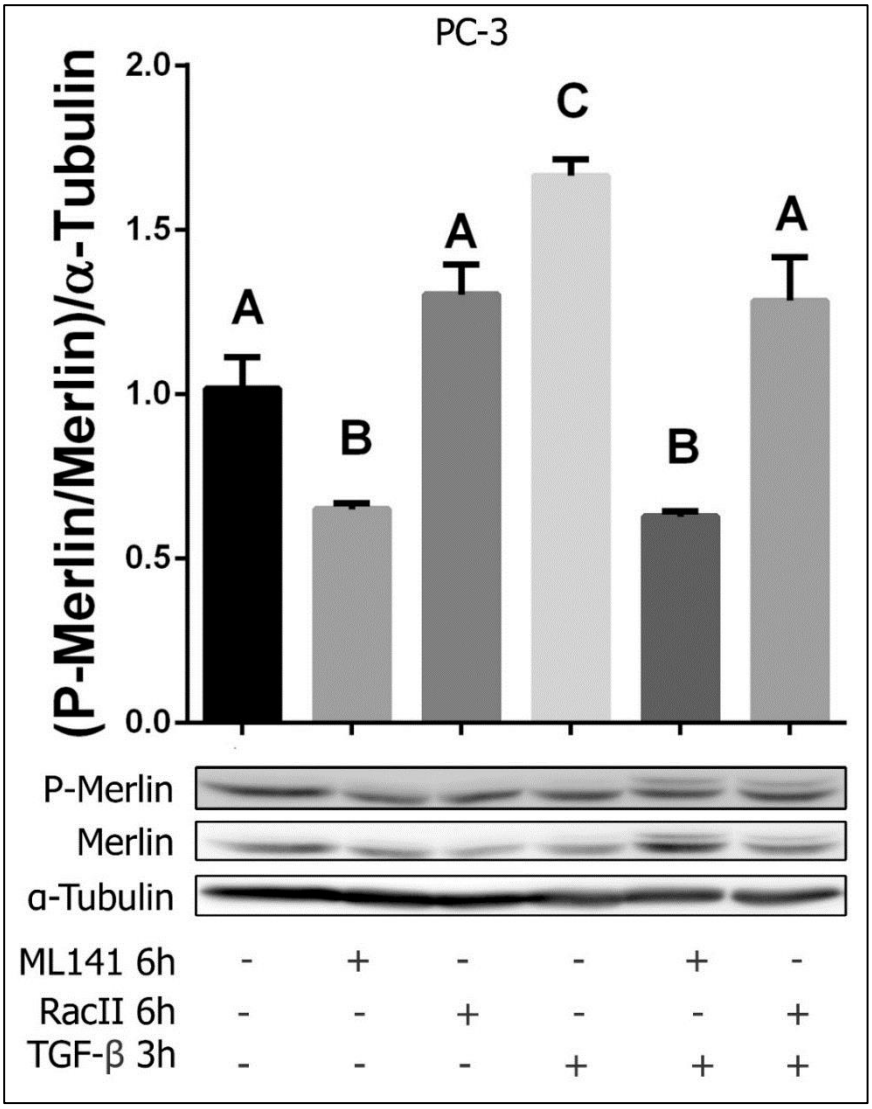

Figure 3. 15 - TGF-β effect on the inhibition of Pak2 stimulatory proteins Rac1 and CDC42 in PC-3

Expression levels of P-Merlin compared to total Merlin were normalized with α-Tubulin loading control in PC-3 cells. Immunoblots (n=6) were used to determine P-Merlin levels with ± inhibitors (ML141 & RacII) and stimulated with ± TGF-β. Pixel densities from each immunoblot were analyzed (ANOVA and Tukey's post hoc) to determine significance. Letter designations is to differentiate between different statistical groups.

3.11.3 DU145 Cell Line

With the effectiveness of inhibitors against the Pak2 activators Rac1 and CDC42 showing an inhibition of TGF-β suggesting Pak2 activity in PC-3 cells, in order to test the generalization, I tested another advanced prostate cancer cell, DU145. P-Merlin levels were measured and compared against total amount of Merlin normalised to α-Tubulin, the effect of Rac1 inhibitors (RacII) and CDC42 inhibitor (ML141) ±TGF-β (5ng/ml) was measured (*Figure 3.16*). DU145 cells treated with either ML141 or RacII for 6 hours with or without TGF-β showed a significant reduction in P-Merlin levels in comparison to total amount of Merlin in the untreated cells. Consistent with previous findings (*Figure 3.13*), DU145 cells treated with TGF-β for 3 hours showed a significant increase on P-Merlin. Although the results for DU145 are similar to those of PC-3 in that ML141 dramatically decreased steady state levels of P-Merlin, unique to this cell line was that not only did RacII cause a similar decrease, but that both inhibitors further reduce P-Merlin levels in the presence of TGF-β. Although the ratio of CDC42/Rac1 observed in figures 3.3 vs 3.4 showed a dominance in CDC42, the total amount of CDC42/Rac1 in DU145 cells is significantly less than the other prostate cancer cell lines (*Figure 3.2*) making both inhibitors effective in reducing Pak2 activity.

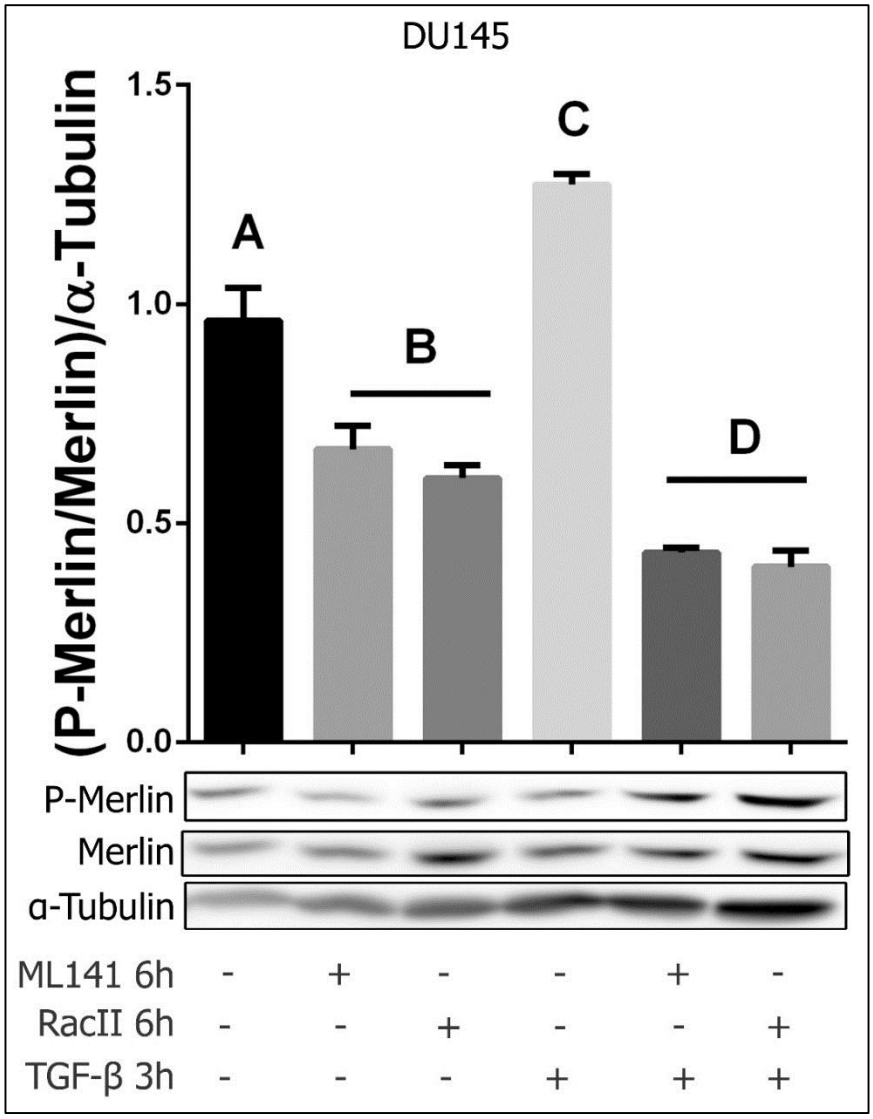

Figure 3. 16 - TGF-β effect on the inhibition of Pak2 stimulatory proteins Rac1 and CDC42 in DU145 cells

Expression levels of P-Merlin compared to total Merlin were normalized with α-Tubulin loading control in DU145 cells. Immunoblots (n=6) were used to determine P-Merlin levels with ± inhibitors (ML141 & RacII) and stimulated with ± TGF-β. Pixel densities from each immunoblot were analyzed (ANOVA and Tukey's post hoc) to determine significance. Letter designations is to differentiate between different statistical groups.

3.12 Migration assay in highly metastatic prostate cancer cell lines

As observed in previous results (Section 3.11), inhibition of the Pak2 stimulatory proteins Rac1 and CDC42 (RacII and ML141, respectively), in advanced prostate cancer cell lines DU145 and PC-3, stopped the effect generated by TGF-β in promoting Pak2 activation (Merlin phosphorylation). Active Pak2 and CDC42 have previously been shown to be involved in the promotion of invasion and migration in epithelial cancers such as prostate and ovarian (Goc et al., 2012; Siu et al., 2010). Since our observations that steady state Pak2 activity is higher in advanced prostate cancer cell lines and that TGF-β increases P-Merlin, suggesting that Pak2 activity is increased, we wish to determine the role of TGF-β on Pak2 in a functional cell migration assay.

3.12.1 PC-3 Cell Line

In order to determine the roles of TGF-β and Pak2 in prostate cancer cell migration the Pak2 inhibitor (Frax1036) and Pak2 promoter protein CDC42 inhibitor (ML141) were used to determine if Pak2 promoted migration in prostate cancer via a wound healing assay. Since CDC42 itself is thought to promote cell migration independent of Pak2 (Raftopoulou and Hall, 2004), the use of both inhibitors allowed us to determine the relative contributions of Pak2 activity in CDC42 regulated migration. PC-3 cell migration was measured in the presence of ML141, Frax1036, with or without TGF-β (5ng/ml) for 12 hours (*Figure 3.17*). TGF-β treatment alone promoted the migration of PC-3 cells, while treatment with Frax1036 or ML141 significantly reduced migration 20% ± 4. Either of the inhibitors in combination with TGF-β reduced the effect of TGF-β alone.

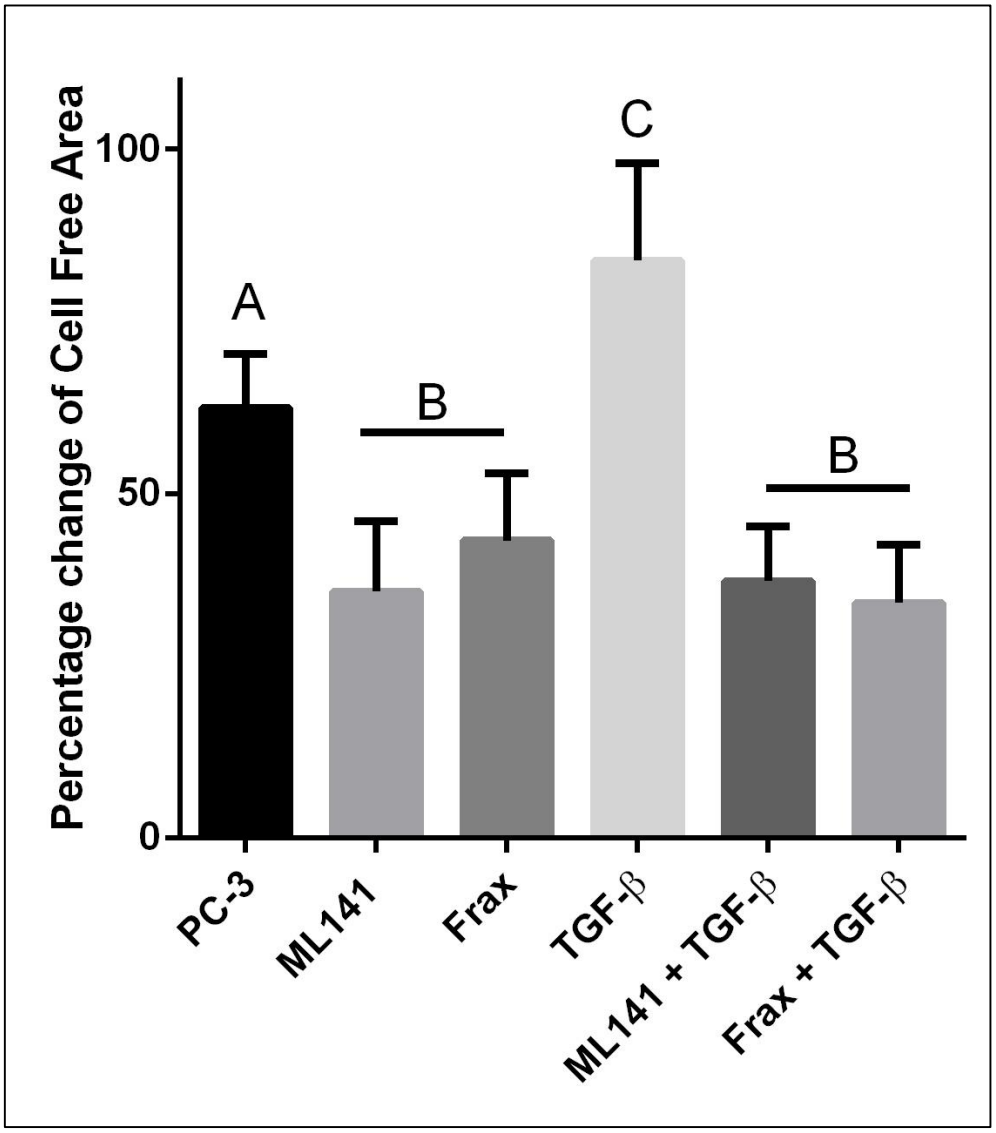

Figure 3. 17 - Migration assay in highly metastatic PC-3 cell line

PC-3 migration with ± inhibitors (ML141 & Frax1036) and stimulated with ± TGF-β (n=8) for 12 hours. Pixel densities from each cell free area picture were analyzed (ANOVA and Tukey's post hoc) to determine significance. Letter designations is to differentiate between different statistical groups.

3.12.2 DU145 Cell Line

As observed in previous results the effect of Pak2 inhibitors significantly reduced PC-3 cell migration (*Figure 3.17*), in order to determine if the Pak2 inhibitor (Frax1036) and Pak2 promoter protein CDC42 inhibitor (ML141) show similar results to TGF-β and Pak2 promoted migration in prostate cancer via a wound healing assay in DU145 was assessed. DU145 cell migration was measured in the presence of ML141, Frax1036, with or without TGF-β (5ng/ml) for 12 hours (*Figure 3.18*). TGF-β treatment alone promoted the migration of DU145 cells ($p<0.05$), while treatment with Frax1036 significantly reduced migration by 23% ($p<0.0001$). Either inhibitor in combination with TGF-β removed the stimulated effect generated by TGF-β alone (ML141 $p<0.0001$; Frax1036 $p<0.0001$). the effect of Frax1036 with or without TGF-β suggest much of DU145 cells inherent migration ability is stimulated by its increased basal Pak2 activity. This data is also consistent with previous data (*Figure 3.13*), showing an increasing effect of TGF-β + ML141 on Pak2 activity (P-Merlin). Although ML141 and TGF-β + ML141 were not statistically different there was a decrease making TBF-β + ML141 different from no treatment.

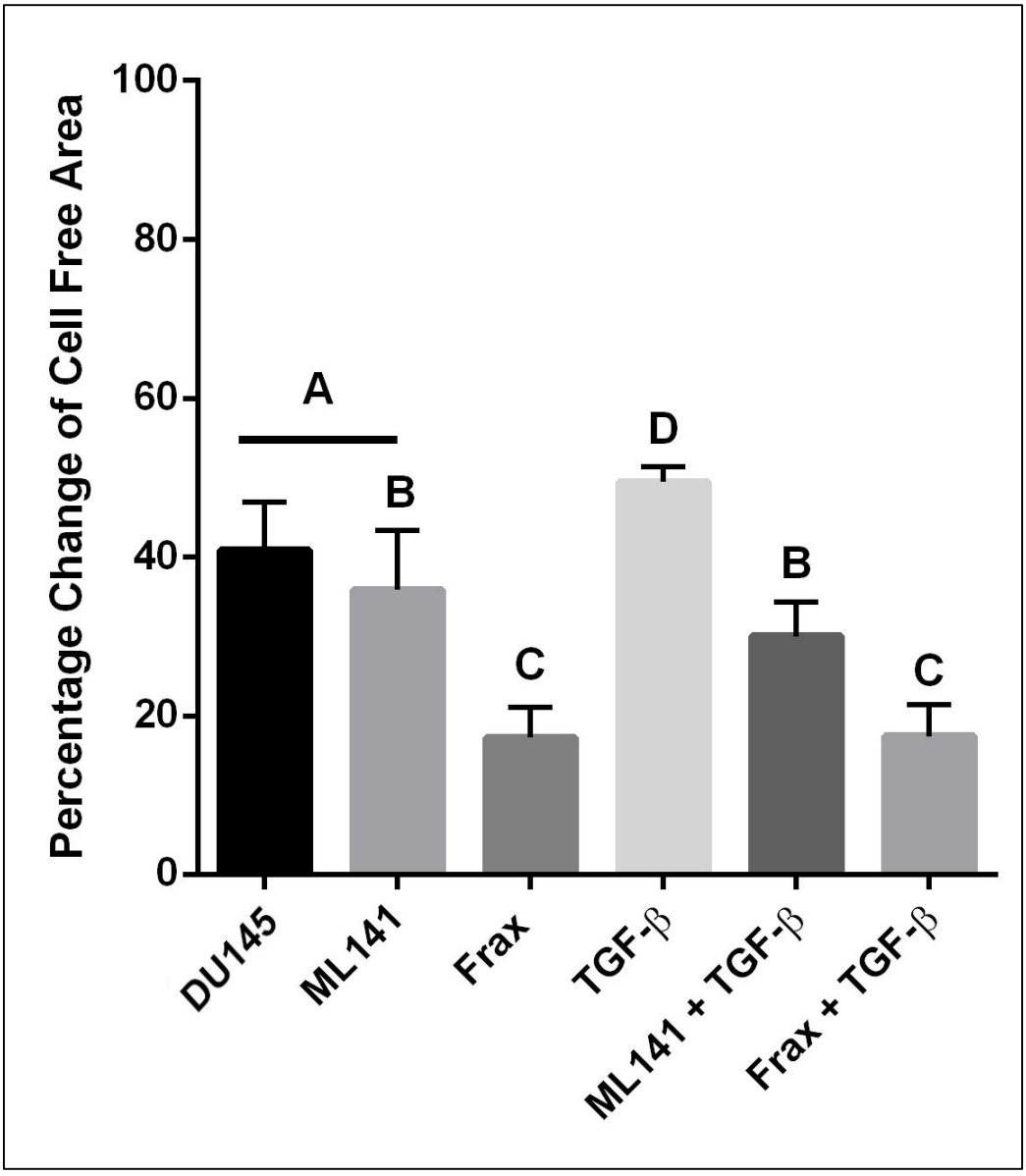

Figure 3. 18 - Migration assay in highly metastatic DU145 cell line

DU145 migration with ± inhibitors (ML141 & Frax1036) and stimulated with ± TGF-β (n=8) for 12 hours. Pixel densities from each cell free area picture were analyzed (ANOVA and Tukey's post hoc) to determine significance. Letter designations is to differentiate between different statistical groups relative to untreated.

3.12.3 RWPE-1 Cell Line

With the observations of previous experiments (Section 3.12.1 and 3.12.2) inhibitors Frax1036 or ML141 having an effect in reducing the migration of advanced prostate cancer cell lines PC-3 and DU145, and negating the stimulated effect of TGF-β. The use of the normal prostate cell line RWPE-1 as a comparison for the prostate cancer cell lines. RWPE-1 cell migration was measured in the presence of ML141, Frac1036, with or without TGF-β (5ng/ml) for 12 hours (*Figure 3.19*). As observed previously (*Figure 3.*13) TGF-β treatment has no effect on the migration of RWPE-1 cells, while the Pak2 inhibitor Frax1036 significantly reduced the migration of RWPE-1 cells. The combination of Frax1036 in the presence of TGF-β has the same effect as Frax1036 alone. The normal prostate cell line RWPE-1 behaved as a normal epithelial cell should, having low inherent migratory capacities, needing Pak2 activity for limited migration not stimulated by TGF-β (Rangwala et al., 2005; Wilkes et al., 2009).

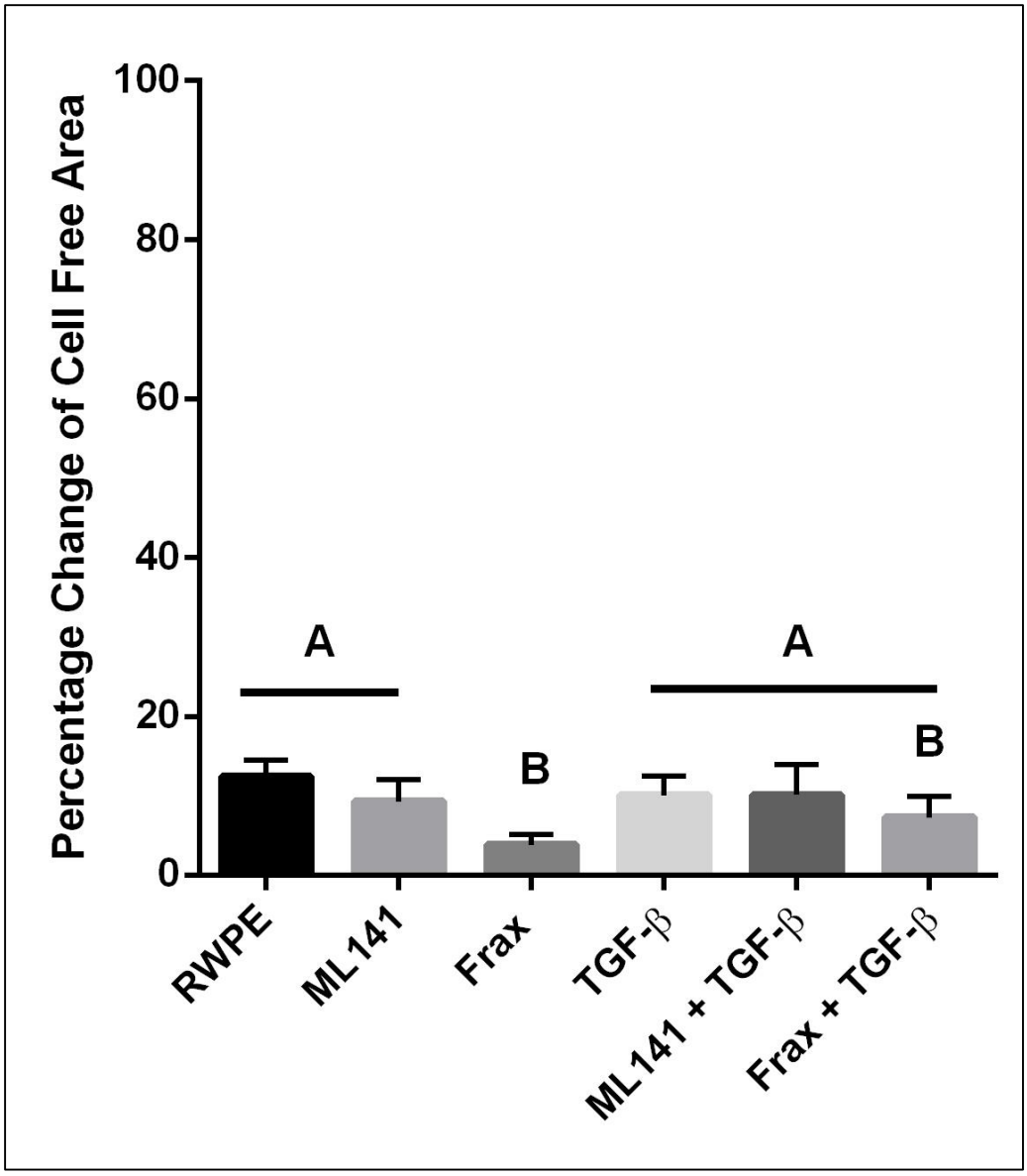

Figure 3. 19 - Migration assay in normal epithelial cell line RWPE-1

RWPE migration with ± inhibitors (ML141 & Frax1036) and stimulated with ± TGF-β (n=8) for 12 hours. Pixel densities from each cell free area picture were analyzed (ANOVA and Tukey's post hoc) to determine significance. Letter designations is to differentiate between different statistical groups.

Chapter IV Discussion

TGF-β is a member of a family of cytokines that control numerous cellular functions including cell migration, proliferation, differentiation, apoptosis and EMT (Grant and Kyprianou, 2013; Massagué, 2008). Both epithelial and mesenchymal cells possess the TGF-β canonical Smad signaling cascade. However, epithelial cells are growth inhibited, while mesenchymal cells are growth stimulated by TGF-β, suggesting a difference in the signaling mechanism between cell types.

In normal epithelial cells, TGF-β stops the cell cycle at the G1 stage, induces differentiation, or promotes apoptosis. When an epithelial cell is transformed into a cancer cell, components of the TGF-β signalling pathway may be mutated (Pasche, 2001), making it impossible for TGF-β to negatively control cell replication, leading to its proliferation. To exacerbate the problem, the surrounding stromal cells, respond to TGF-β and proliferate further promoting an increase in their production of TGF-β. TGF-β acts on the surrounding stromal cells, immune cells, endothelial and smooth-muscle to cells, stimulating angiogenesis allowing the cancer cells to be more invasive (Heldin et al., 2009; Principe et al., 2014). In my case the known normal replication times for our cancer cells were 33 hours for PC-3 cells and 34 hours for DU145 (Keer et al., 1990; Rossi and Zetter, 1992) in normal growth medium concentration 10% FCS (multiple growth factors, maximum stimulation) lead to the conclusion that the results observed in the wound healing assays in reduces serum media conditions are due to the migration of the cells and not their replication.

In cancer, TGF-β has a complex role. Initially, it was identified as a tumor suppressor since it inhibits the growth of epithelial cells and induces apoptosis (Nguyen and Pollard, 2000). However, at later stages of tumor progression TGF-β acts as a tumor promoter (Xie et al., 2002).

At a later stage of the disease, the tumor cells lose their ability to be growth arrested by TGF-β but retain their ability to undergo EMT, which correlates to increased invasiveness and metastasis (Kingsley et al., 2007). My data is consistent with this concept that in advanced prostate cancer cells I found that TGF-β not only stimulated an already elevated Pak2 activity but this translated to increased mobility of these models of advanced disease.

Pak2 activation by TGF-β is a process that occurs normally in mesenchymal cells, but it is not a normal event in epithelial cells. TGF-β induced Pak2 activation is necessary for the morphological alterations and proliferative responses induced in mesenchymal cells, such as cytoskeletal rearrangement associated with lamellipodia or filopodia and cell migration (Hough et al., 2012; Jaffer and Chernoff, 2002; Wilkes et al., 2003). Group A Paks are a major downstream effector of the small GTPases Rac1 and CDC42, which are involved in the actin-based cytoskeletal remodeling. Group A Paks bind to CDC42 and Rac1 through a GTPase binding domain (Renkema and Pulkkinen, 2002).

Rac1, Cdc42 and Pak proteins are important for physiological responses to growth factors in normal epithelial cells, such as cell migration, cell adhesion and cytoskeletal remodeling (Somanath and Byzova, 2009). These GTPases have been shown to be involved in the promotion of invasion and migration in prostate cancer and ovarian cancer cells by regulating microtubule dynamics, adhesion and post-mitotic spreading in fibroblasts (Goc et al., 2012; Siu et al., 2010). With TGF-β stimulating Pak2 activity in fibroblast and epithelial cancers including EMT, we decided to investigate if TGF-β activation of Pak2 may be involved in prostate cancer cell migration.

4.1 Pak2 protein expression levels in Prostate Cancer

The Pak family of kinase enzymes are involved in multiple physiological responses in normal epithelial cells, but they are also involved in the promotion of invasion and migration in cancers such as ovarian and prostate cancer (Goc et al., 2012; Siu et al., 2010; Somanath and Byzova, 2009). Pak2 activation results from the interactions of the small GTPases, Rac1 and CDC42 with inactive Pak2, through the interactions of TβRI and TβRII receptors with TGF-β, PI3K is activated recruiting Rac1 and CDC42 to interact with Pak2. In all cancer cells elevated P-Merlin and elevated TGF-β are indicators of Pak2 activation.

As an initial step to elucidate the role(s) of Pak signalling in prostate cancer migration, we determined protein levels of its pathway components. Pak2 protein expression levels were measured in a panel of prostate cancer cells corresponding to the progression of the disease (primary tumor: 22RV-1, early Tumor: LNCaP, and late tumor: PC-3 and DU145) and compared to a non-malignant control RWPE. The prostate cancer cell lines LNCaP and DU145 had similarly lower Pak2 protein levels in comparison to the non-malignant control RWPE. Although there are no studies defining Pak2 protein levels in prostate cancer, a recent study has shown increased levels of Pak2 phosphorylation, as well as mRNA in castration resistant cancer cells (Jiang et al., 2015). There is evidence in ovarian cancer that Pak2 levels remain similar in the normal ovarian cells compared to the ovarian cancer cells (Siu et al., 2010). My results (*Figures 3.1, 3.17, and 3.18*) together with this data suggests that the reduced levels of Pak2 observed in prostate cancer cells lines are biologically relevant.

4.2 Expression of Pak2 stimulators Rac1 and CDC42

The activation of the group A Paks results from the interaction of the Rho GTPase proteins Rac1 and CDC42 with the p21-binding domain (PDB), making this Pak family its major downstream effector (Jaffer and Chernoff, 2002; Lei et al., 2000). Although Rac1 activation promotes prostate cancer motility and migration (Goc et al., 2012), the amount necessary to promote cancer motility and migration is unknown. My analysis of the total amount of Rac1 and CDC42 show significantly lower levels of both proteins in all prostate cancer cell lines, especially in the later stage tumor cell DU145 in comparison to the control RWPE-1. Previous studies have reported that Pak2 overexpression or aberrant activation by Rac1 or CDC42 generates oncogenic effects in cells, including the acquisition of growth signaling autonomy, evasion of apoptosis and the promotion of invasion and metastasis (Radu et al., 2014). Since my results show that the total amount of Rac1 and CDC42 present in prostate cancer cells is significantly less than in normal prostate epithelial cells, the next step was to determine if a difference in either was present. Comparatively, Rac protein levels were lower in prostate cancer cells compared to RWPE-1, while protein levels of CDC42 increased in the prostate cancer cell lines representing the later stages of the disease. My results suggest that the advanced prostate cancer cells, PC-3 and DU145, show a dominance of CDC42 over Rac1. Although, both Rac1 and CDC42 are required for Pak2 activation (Jaffer and Chernoff, 2002; Lei et al., 2000) and both of them are considered to be involved in regulating migration and invasion of cancer (Guo et al., 2003), it is not clear which one of them is primarily responsible for Pak activation. These results indicate that within the metastatic prostate cancer cells the ratio of Rac1 to CDC42 turn in favor for CDC42, suggesting a preference in the advance prostate cancer cell lines PC-3 and DU145 for the use of CDC42 to induce Pak2 activation and be involved in their migration.

The relationship between protein abundance and mRNA expression is not fully understood. Protein levels could be different due to changes in the rate of protein synthesis, mRNA or degradation. There are reports demonstrating that the regulatory processes controlling the steady-state protein abundance change under different cellular conditions (Greenbaum and Colangelo, 2003; Vogel and Marcotte, 2012). The following qPCR analysis indicated that expression of Rac1 is elevated in the prostate cancer cell lines LNCaP and PC-3, in comparison to the control. While the gene expression of CDC42 is elevated only in PC-3.

4.3 Expression levels of Pak2 inhibitors Erbin and Merlin

Pak2 activation is due to the interactions of the Rho GTPases Rac1 and CDC42. Pak2 inhibition has been reported to be achieved by the interaction of Erbin and Merlin complexes binding and inactivating GTPase-bound Pak2 in epithelia (Rangwala et al., 2005; Wilkes et al., 2009). The outcome of interaction of the Erbin/Merlin complex depends upon the cell context. For instance, in fibroblasts Pak2 provides growth stimulatory signals and Merlin becomes phosphorylated and inactivated likely due to the lower levels of Erbin protein expression (McClatchey and Giovannini, 2005; Wilkes et al., 2009). However, in epithelial cells increased Pak2 activity results in cell death (Yan et al., 2012). The Erbin/ Merlin complex disrupts Pak2 interaction with Rac1 and CDC42 resulting in the inactivation of Pak2 (Rangwala et al., 2005; Wilkes et al., 2009). My data showed a dramatic reduction in Erbin protein, similar to that seen in fibroblasts when compared to epithelial cells (Wilkes et al., 2009). This indicates that the prostate cancer cells share more similar expression patterns to fibroblast than epithelial cells with respect to Erbin.

Merlin protein expression levels measured by immunoblots, showed levels were significantly higher in all prostate cancer cells compared to the control. Like Erbin, Merlin gene expression levels follow a similar pattern as the protein levels, showing elevated levels in the prostate cancer cells 22RV-1, LNCaP, and PC-3 in comparison to the control RWPE-1. As previously described, a difference between protein abundance and mRNA expression does not necessarily correlate with the protein steady-state levels (Greenbaum and Colangelo, 2003; Vogel and Marcotte, 2012). Erbin and Merlin protein expression levels in all prostate cancer cell lines display a difference in the ratio similar to that shown previously in fibroblast (Wilkes et al., 2009), suggesting that the panel of prostate cancer cells are following in a similar protein expression profile to mesenchymal and not epithelial cells.

4.4 Pak2 activity promotes Merlin phosphorylation

Tumor suppressor Merlin is a protein reported to show two interactions with Pak2. As an inhibitor for Pak2 activity, the Merlin/Erbin complex disrupts Pak2 interaction with the GTPases Rac1 and CDC42 (Kissil et al., 2003; Rangwala et al., 2005). Merlin also acts as a direct substrate for Pak2, becoming phosphorylated at the serine 518. This phosphorylation impairs Merlin function and leads Merlin to its degradation (Kissil et al., 2002; Wilkes et al., 2009; Xiao et al., 2002). Merlin localization in the adherent junctions and its interaction with components of these junctions suggest the involvement of Merlin in controlling them. The loss or inactivation of Merlin may be involved in the development of tumor metastasis (Bretscher et al., 2002; Lallemand et al., 2003), since phosphorylation of Merlin by Pak2 inactivates Merlin growth suppressive functions (Xiao et al., 2002; Rong et al., 2004).

Since Merlin has been shown to be a Pak2 substrate (McClatchey and Giovannini, 2005) steady state Pak2 activity levels were implied by measuring P-Merlin levels with immunoblots representing a panel of prostate cancer cells (22RV-1, LNCaP, PC-3, and DU145) compared to a non-malignant control RWPE-1. The levels of P-Merlin, across the panel of prostate cancer cells representing progression of the disease, showed higher levels of P-Merlin at PC-3 and DU145 cell lines suggesting a higher basal Pak2 activity. These results suggest that Pak2 is more active in advanced prostate cancer cells PC-3 and DU145 suggesting its ability to promote the malignancy of these cells. My results show that not only did P-Merlin levels increase in androgen independent cell lines (advanced disease), but that TGF-β further increased P-Merlin levels, suggesting that TGF-β can promote prostate cancer metastasis through its inactivation of Merlin.

4.5 PI3K pathway responsiveness to TGF-β

TGF-β is an important cytokine that possesses multiple functions, however its activity is cell type specific. For instance, in normal epithelial cells, TGF- β stops proliferation and promotes apoptosis, while in mesenchymal cells it promotes cell growth through the activation of Pak2 via the PI3K pathway (Heldin et al., 2009; Wilkes et al., 2009; Hough et al., 2012; Principe et al., 2014). It has been previously reported that TGF-β does not promote the activation of the PI3K pathway in epithelial cancers (Wilkes et al., 2003), but the cell activation of the PI3K pathway promotes AKT and ERK activation to enhance cancer motility and invasiveness (Dumont et al., 2003).

Our previously discussed data (Merlin/Erbin ratio being similar to fibroblast) and an increased basal Pak2 activity (*Figure 3.7*) all suggests that if EMT alters signalling in these cells,

and TGF-β no longer inhibits their growth, it may activate Pak2. In order to evaluate the responsiveness of the PI3K pathway to TGF-β, immunoblots were prepared with samples of the prostate cancer cells and the control RWPE-1. The samples were treated with TGF-β for different periods of time (0 hours, 1 hours, and 3 hours), and checked for P-GSK-3β levels to confirm AKT activity and P-ERK levels to imply Pak2 activation as was shown in mesenchymal versus epithelial cells (Hough et al., 2012; Wilkes et al., 2005).

The prostate cancer cells 22RV-1 and PC-3 showed no variation in P-GSK-3β levels indicating that TGF-β did not promote activation of the AKT arm of the PI3K pathway. TGF-β treatment increased P-ERK levels in 22RV-1 and DU145 prostate cancer cells suggesting the activation of Pak2 by TGF-β. Interestingly, as seen in the *Appendix A1*, treatment with TGF-β did not promote ERK phosphorylation in PC-3 prostate cancer cells and non-malignant control RWPE-1. In order to confirm if the pathway is functional, treatment with EGF caused phosphorylation of ERK indicating that the pathway is functional, and not stimulated by TGF-β (Sheikh et al., 2004). PC-3 cells behave in a similar manner to the non-malignant epithelial control RWPE-1 in response to ERK phosphorylation stimulated by EGF, indicating that the normal response to TGF-β can remain partially intact even in some advanced prostate cancers.

4.6 TGF-β promotes Pak2 activity in prostate cancer

The phosphorylation of ERK, in prostate cancer cells, in response to TGF-β suggest that TGF-β activates Pak2. Our lab has previously identified ERK as a downstream target of activated Pak2 (Hough et al., 2012). In this study, I showed an increase in steady state levels of P-Merlin with advanced disease related cell lines (*Figure 3.7 B*), suggesting steady state Pak2 activity is increased with disease progression. As a measure of Pak2 activity, I checked for

differences in Merlin phosphorylation (S518) to indicate Pak2 activity, since this site has previously shown to be a target of activated Pak2 (Kissil et al., 2002).

Since Pak2 is capable of inducing ERK phosphorylation in response to TGF-β, prostate cancer cells were treated with TGF-β for different periods of time and P-Merlin levels were measured by an immunoblot to provide evidence that TGF-β promoted Pak2 activation. The non-malignant control RWPE-1 showed no variation of P-Merlin levels with TGF-β treatments, consistent with previous reports indicating that TGF-β does not promote Pak2 activity on normal epithelial cells (Wilkes et al., 2003; Heldin et al., 2009; Principe et al., 2014). Interestingly, all prostate cancer cells were able to respond to TGF-β (22RV-1, PC-3, and DU145) and showed increased levels of P-Merlin by 3 hours of TGF-β treatment. These results suggest that TGF-β stimulates Pak2 activity at all stages of the disease interpreted by the panel of prostate cancer cells showing primary tumor and late tumor cells which means that Pak2 activation by TGF-β could enhance the malignancy of the cells.

4.7 Inhibitors for Rac1 and CDC42 enables TGF-β promoted Pak2 activity

As previously mentioned, results demonstrated the promotion of Pak2 activity by TGF-β treatment in the prostate cancer cells: 22RV-1, PC-3, and DU145 (*Figure 3.11 – 3.13*). To further address the role of Pak2 in transducing the TGF-β signal to Merlin and possibly generating the detrimental effect of TGF-β in prostate cancer (Massagué, 2008; Siu et al., 2010), P-Merlin levels were measured in the presence of inhibitors of Pak2 promoters, Rac1 (RacII) and CDC42 (ML141). The effectiveness of Pak2 inhibition in the presence of exogenous TGF-β was tested. The analysis of P-Merlin levels in the non-malignant control RWPE-1 cells suggest that TGF-β does not promote Pak2 activity in normal cells, as expected both inhibitors showed a

reduction on P-Merlin levels indicating their effectiveness at hindering basal Pak2 activity. In the advanced stage prostate cancer cells: PC-3 and DU145, it was confirmed that TGF-β promoted Pak2 activity as previously showed (*Figure 3.15 - 3.16*). For PC-3 cells, Rac1 inhibitor negated this effect, and for DU145 cells both inhibitors reduced Pak2 activity and showed to negate the effect generated by TGF-β in promoting Pak2 activity. Inhibition of Pak2 with the application of CDC42 inhibitor ML141 showed promising results for cancelling the effects generated by TGF-β in advanced prostate cancer cells PC-3 and DU145. These results indicate that inhibition of the Pak2 activator CDC42 can negate the effects generated by TGF-β in advanced prostate cancer cells PC-3 and DU145. While there is more to understand and confirm about the cellular effects of inhibiting Pak2, this results suggest that the inhibition of Pak2 could be used as therapeutic drug to negate the effects generated by TGF-β in prostate cancer. Although there are differences in the responses observed in PC-3 and DU145 cells to Rac1 and CDC42 inhibitors, in previous results DU145 cells possess much less Rac1 and CDC42 than PC-3 cells (*Figure 3.2*), with DU145 showing a dominance in preference to CDC42, but both cells are driven by Pak2 activation.

4.8 Migration assay in highly metastatic prostate cancer cell lines

TGF-β promotes growth and migration in advanced stages of prostate cancer (Al-Azayzih et al., 2015; Massagué, 2008), the mechanism involved in promoting the cancer migration is not completely understood. Previous results (Section 3.11) confirm the effectiveness of hindering Pak2 activity promoted by TGF-β using an inhibitor for one of Pak2 promotor proteins CDC42 (ML141). The next experiments (Section 3.12) assessed the impact of Pak2 inhibition on the migration of prostate cancer cells.

The effect of Pak2 inhibitor Frax1036 and CDC42 inhibitor ML141 was measured in a wound healing assay on the highly metastatic prostate cancer cell lines PC-3 and DU145. Analysis of the percentage of cell free area demonstrated that Pak2 inhibitor Frax1036 significantly slowed the migration of DU145 cells in a 12 hours treatment and both inhibitors showed the reduced migration effect on PC-3 cells. Treatment with TGF-β resulted in an increased migration of PC-3 and DU145 cells. Interestingly as seen in *Appendices A2 and A3*, the combination of ML141 or Frax1036 inhibitors, with TGF-β, resulted in the complete suppression of the TGF-β mediated migration. The inhibition of Pak2 with either CDC42 inhibitor ML141 or Frax1036 resulted in the reduction of both endogenous migration and elimination of TGF-β mediated migration in advanced prostate cancer cells PC-3 and DU145.

As a control, the migration assay was performed in the prostate normal epithelial cell line RWPE-1 (*A4*), confirming that epithelial cells do not migrate in the presence of Pak2 or with the stimulation of TGF-β, also confirming that the effect of the inhibitors (Frax1036 and ML141) have no effect on normal prostate epithelial cells compared to the effect they have in prostate cancer cells. With the used of inhibitors (ML141 and Frax1036) targeting Pak2, we discovered that is possible to stop the promoted migration generated by TGF-β in advanced metastatic prostate cancer cells, suggesting that the use of this type of inhibitor could become another tool in the treatment for prostate cancer. Although these results only reflect cellular data, the replication times for PC-3 cells (33 hours) and DU145 cells (34 hours) in full serum media indicate that the observation obtain in the migration assay performed under reduce serum media conditions (1% vs 10%) indicate the efficacy of the inhibitors in disrupting cell migration generated by Pak2 activity, there is more to understand of their effect in animal models before the inhibitors could be used in humans.

4.9 Conclusions

The main purpose of this study was to assess the involvement of Pak2 in regulating aberrant prostate cancer cell migration. Results indicated that all prostate cancer cell lines studied display a dysregulation of the regulators of Pak2 corresponding with disease progression. There is a shift in the ratio of stimulatory proteins, with a dominance of CDC42 corresponding to disease progression. The ratio of Merlin to Erbin is altered at all stages of disease. Together this indicates a dysregulation of both stimulators and inhibitors that results in an increase in basal Pak2 activity, confirmed by the increase in P-Merlin levels corresponding to progression of the disease. Additionally, this increased Pak2 activity is further stimulated by TGF-β in all stages of the disease, while inhibition of Pak2 prevents both endogenous and TGF-β promoted migration of advanced prostate cancer cell lines PC-3 and DU145. In both cases the effect of CDC42 on migration could be accounted for Pak2 actions. Additional experiments such as a comparison of the effect generated by TGF-β in promoting Pak2 activation in a prostate cancer cells, compared the efficacy of ML141 and Frax1036 inhibitors in animal models and in tumor samples would be necessary to develop and prove the effectiveness of an inhibitor that could potentially be used in the future as treatment for advanced prostate cancer.

References

1. Abate-Shen, C., Shen, M.M., 2000. Molecular genetics of prostate cancer. Genes & Development 14, 2410–2434.
2. Al-Azayzih, A., Gao, F., Somanath, P.R., 2015. P21 activated kinase-1 mediates transforming growth factor β1-induced prostate cancer cell epithelial to mesenchymal transition. Biochim. Biophys. Acta 1853, 1229–39.
3. Bakin, AV, Tomlinson, AK, Bhowmick, NA, 2000. Phosphatidylinositol 3-kinase function is required for transforming growth factor β-mediated epithelial to mesenchymal transition and cell migration. Journal of Biological Chemistry 275, 36803-36810.
4. Bianchi AB1, Hara T, Ramesh V, Gao J, Klein-Szanto AJ, Morin F, Menon AG, Trofatter JA, Gusella JF, Seizinger BR., 1994. Mutations in transcript isoforms of the neurofibromatosis 2 gene in multiple human tumour types. Nature Genetics. 6, 185-192.
5. Blanchette, F., Rivard, N., Rudd, P., Grondin, F., Attisano, L., Dubois, C., 2001. Cross-talk between the p42/p44 MAP Kinase and Smad Pathways in Transforming Growth Factor β1-induced Furin Gene Transactivation. J Biol Chem 276, 33986–33994.
6. Bokoch, G.M., 2003. Biology of the p21-activated kinases. Annu. Rev. Biochem. 72, 743–81.
7. Borg, J.-P., Marchetto, S., Bivic, A., Ollendorff, V., Jaulin-Bastard, F., Saito, H., Fournier, E., Adélaïde, J., Margolis, B., Birnbaum, D., 2000. ERBIN: a basolateral PDZ protein that interacts with the mammalian ERBB2/HER2receptor. Nat Cell Biol 2, 407–414.
8. Bostwick, D., 2000. Prostatic intraepithelial neoplasia. Curr Urology Reports 1, 65–70.
9. Brawley, O., 2012. Prostate cancer epidemiology in the United States. World J Urol 30, 195–200.

10. Bretscher, A., Edwards, K., Fehon, R.G., 2002. ERM Proteins and Merlin: Integrators at the Cell Cortex. Narute Reviews Molecular Cell Biology 3, 586–599.
11. Broeke, C. et al. Alphaherpesvirus US3-mediated reorganization of the actin cytoskeleton is mediated by group A p21-activated kinases. Proceedings of the National Academy of Sciences 106, 8707–8712 (2009).
12. Bubendorf, L, Schöpfer, A, Wagner, U, Sauter, G, Moch, H, 2000. Metastatic patterns of prostate cancer: an autopsy study of 1,589 patients. Human pathology.
13. Buijs, JT, van der Pluijm, G, 2009. Osteotropic cancers: from primary tumor to bone. Cancer letters.
14. Buijs, J., Henriquez, N., van Overveld, P., van der Horst, G., ten Dijke, P., van der Pluijm, G., 2007. TGF-β and BMP7 interactions in tumour progression and bone metastasis. Clin Exp Metastas 24, 609–617.
15. Canadian Cancer Society's Advisory Committee on Cancer Statistics, 2015. Canadian Cancer Statistics 2015. Toronto, ON.
16. Carlin, BI, Andriole, GL, 2000. The natural history, skeletal complications, and management of bone metastases in patients with prostate carcinoma. Cancer.
17. Dai, F., Chang, C., Lin, X., Dai, P., Mei, L., Feng, X.-H., 2007. Erbin inhibits transforming growth factor signaling through a novel Smad-interacting domain. Molecular and cellular biology 27, 6183–6194.
18. Deweerdt, S., 2015. Prognosis: Proportionate response. Nature 528, S124–S125.
19. Dumont, N., Bakin, A.V., Arteaga, C.L., 2003. Autocrine transforming growth factor- signaling mediates Smad-independent motility in human cancer cells. Journal of Biological Chemistry 278, 3275–3285.

20. Franzén, P., ten Dijke, P., Ichijo, H., Yamashita, H., Schulz, P., Heldin, C.-H., Miyazono, K., 1993. Cloning of a TGFβ type I receptor that forms a heteromeric complex with the TGFβ type II receptor. Cell 75, 681–692.
21. Goc, A, Abdalla, M, Al-Azayzih, A, Somanath, PR, 2012. Rac1 activation driven by 14-3-3ζ dimerization promotes prostate cancer cell-matrix interactions, motility and transendothelial migration. PloS one.
22. Golovnina, K., Blinov, A., Akhmametyeva, E., Omelyanchuk, L., Chang, L.-S., 2005. Evolution and origin of merlin, the product of the Neurofibromatosis type 2 (NF2) tumor-suppressor gene. Bmc Evol Biol 5, 1–18.
23. Grant, C.M., Kyprianou, N., 2013. Epithelial mesenchymal transition (EMT) in prostate growth and tumor progression. Transl Androl Urol 2, 202–211.
24. Greenbaum, D, Colangelo, C, 2003. Comparing protein abundance and mRNA expression levels on a genomic scale. Genome Biology 4, 117-125.
25. Greenburg, G, Hay, ED, 1982. Epithelia suspended in collagen gels can lose polarity and express characteristics of migrating mesenchymal cells. The Journal of cell biology.
26. Grimes, CA, Jope, RS, 2001. The multifaceted roles of glycogen synthase kinase 3β in cellular signaling. Progress in neurobiology.
27. Guo, F, Gao, Y, Wang, L, Zheng, Y, 2003. p19Arf-p53 tumor suppressor pathway regulates cell motility by suppression of phosphoinositide 3-kinase and Rac1 GTPase activities. Journal of Biological Chemistry.
28. Guo, X., Ramirez, A., Waddell, D.S., Li, Z., Liu, X., Wang, X.-F., 2008. Axin and GSK3-control Smad3 protein stability and modulate TGF- signaling. Genes & development 22, 106–120.

29. Hamaratoglu F1, Willecke M, Kango-Singh M, Nolo R, Hyun E, Tao C, Jafar-Nejad H, Halder G., 2006. The tumour-suppressor genes NF2/Merlin and Expanded act through Hippo signalling to regulate cell proliferation and apoptosis. Nature cell Biology. 8, 27-36.

30. Heinlein, C.A., Chang, C., 2004. Androgen Receptor in Prostate Cancer. Endocrine Reviews 25, 276–308.

31. Heldin, C.-H.H., Landström, M., Moustakas, A., 2009. Mechanism of TGF-beta signaling to growth arrest, apoptosis, and epithelial-mesenchymal transition. Curr. Opin. Cell Biol. 21, 166–76.

32. Hodson, R., 2015. Small organ, big reach. Nature 528, S118–S119.

33. Horoszewicz, JS, Leong, SS, Kawinski, E, Karr, JP, 1983. LNCaP model of human prostatic carcinoma. Cancer research.

34. Hough, C, Radu, M, Doré, J., 2012. Tgf-beta induced Erk phosphorylation of smad linker region regulates smad signaling. PloS one.

35. Hough, C., Radu, M., Doré, J., 2012. TGF-Beta Induced Erk Phosphorylation of Smad Linker Region Regulates Smad Signaling. Plos One 7, e42513.

36. Hu, Y, Chen, H, Duan, C, Liu, D, Qian, L, Yang, Z, Guo, L, 2013. Deficiency of Erbin induces resistance of cervical cancer cells to anoikis in a STAT3-dependent manner. Oncogenesis.

37. Huggins, C., Scott, W.W., Heinen, J.H., 1942. Chemical composition of human semen and of the secretions of the prostate and seminal vehicles. American Journal of Physiology 136, 467–473.

38. Jaffer, ZM, Chernoff, J, 2002. p21-activated kinases: three more join the Pak. The International Journal of Biochemistry & Cell Biology 34, 713-717.

39. Jeong, H.-W.W., Kim, I.-S.S., 2004. TGF-beta1 enhances betaig-h3-mediated keratinocyte cell migration through the alpha3beta1 integrin and PI3K. J. Cell. Biochem. 92, 770–80.

40. Jiang, N., Hjorth-Jensen, K., Hekmat, O., Iglesias-Gato, D., Kruse, T., Wang, C., Wei, W., Ke, B., Yan, B., Niu, Y., Olsen, JV., Flores-Morales, A, 2015. In vivo quantitative phosphoproteomic profiling identifies novel regulators of castration-resistant prostate cancer growth. Oncogene. 34, 2764-2776.

41. Katso, R., Okkenhaug, K., Ahmadi, K., White, S., Timms, J., Waterfield, M.D., 2001. Cellular function of phosphoinositide 3-kinases: implications for development, homeostasis, and cancer. Annu. Rev. Cell Dev. Biol. 17, 615–75.

42. Keer, HN., Kozlowski, JM., Tsai, YC., McEwan, RN., Grayhack, JT., 1990. Elevated transferrin receptor content in human prostate cancer cell lines assessed in vitro and in vivo. The Journal of Urology. 143, 381-5.

43. Kim, IY, Zelner, DJ, Sensibar, JA, Ahn, HJ, Park, L, 1996. Modulation of sensitivity to transforming growth factor-β1 (TGF-β1) and the level of type II TGF-β receptor in LNCaP cells by dihydrotestosterone. Experimental Cell Research 222, 103-110.

44. Kingsley, LA, Fournier, P., Chirgwin, JM, 2007. Molecular Biology of Bone Metastasis. Molecular Cancer Therapeutics 6, 2609-2617.

45. Kissil, JL, Johnson, KC, Eckman, MS, Jacks, T, 2002. Merlin phosphorylation by p21-activated kinase 2 and effects of phosphorylation on merlin localization. Journal of Biological Chemistry 227, 10394-10399.

46. Kissil, JL, Wilker, EW, Johnson, KC, Eckman, MS, 2003. Merlin, the product of the Nf2 tumor suppressor gene, is an inhibitor of the p21-activated kinase, Pak1. Molecular cell.

47. Kozma, R., Ahmed, S., Best, A., Lim, L., 1995. The Ras-related protein Cdc42Hs and bradykinin promote formation of peripheral actin microspikes and filopodia in Swiss 3T3 fibroblasts. Mol. Cell. Biol. 15, 1942–52.

48. Kyprianou, N., English, H.F., Isaacs, J.T., 1990. Programmed cell death during regression of PC-82 human prostate cancer following androgen ablation. The Journal of Cancer Research 50, 3748–3753.

49. Lallemand, D., Curto, M., Saotome, I., Giovannini, M., McClatchey, A.I., 2003. NF2 deficiency promotes tumorigenesis and metastasis by destabilizing adherens junctions. Genes & development 17, 1090–1100.

50. Leevers, S., Vanhaesebroeck, B., Waterfield, M., 1999. Signalling through phosphoinositide 3-kinases: the lipids take centre stage. Curr Opin Cell Biol 11, 219–225.

51. Lei, M., Lu, W., Meng, W., Parrini, M.C., Eck, M.J., Mayer, B.J., Harrison, S.C., 2000. Structure of PAK1 in an autoinhibited conformation reveals a multistage activation switch. Cell 102, 387–97.

52. Li, X., Wen, W., Liu, K., Zhu, F., Malakhova, M., Peng, C., Li, T., Kim, H.-G.G., Ma, W., Cho, Y.Y., Bode, A.M., Dong, Z., Dong, Z., 2011. Phosphorylation of caspase-7 by p21-activated protein kinase (PAK) 2 inhibits chemotherapeutic drug-induced apoptosis of breast cancer cell lines. J. Biol. Chem. 286, 22291–9.

53. Lilja, H., Oldbring, J., Rannevik, G., Laurell, C.B., 1987. Seminal vesicle-secreted proteins and their reactions during gelation and liquefaction of human semen. J. Clin. Invest. 80, 281–5.

54. Lin, H., Wang, X.-F., Ng-Eaton, E., Weinberg, R., Lodish, H., 1992. Expression cloning of the TGF-β type II receptor, a functional transmembrane serine/threonine kinase. Cell 68, 775–785.

55. Long, R.M., Morrissey, C., Fitzpatrick, J.M., Watson, R.W.G., 2005. Prostate epithelial cell differentiation and its relevance to the understanding of prostate cancer therapies. Clin Sci 108, 1–11.

56. Macías-Silva, M., Abdollah, S., Hoodless, P., Pirone, R., Attisano, L., Wrana, J., 1996. MADR2 Is a Substrate of the TGFβ Receptor and Its Phosphorylation Is Required for Nuclear Accumulation and Signaling. Cell 87, 1215–1224.

57. Marzo, A.M., Nakai, Y., Nelson, W.G., 2007. Inflammation, atrophy, and prostate carcinogenesis 25, 398–400.

58. Massagué, J., 2008. TGFbeta in Cancer. Cell 134, 215–30.

59. McClatchey, A., Giovannini, M., 2005. Membrane organization and tumorigenesis—the NF2 tumor suppressor, Merlin. Gene Dev 19, 2265–2277.

60. McNeal, J.E., 1969. Origin and development of carcinoma in the prostate. Cancer 23, 24–34.

61. Moustakas, A., Heldin, C.-H., 2005. Non-Smad TGF-b signals. Journal of cell science 118, 3573–3584.

62. Moustakas, A., Heldin, C.H., 2007. Signaling networks guiding epithelial–mesenchymal transitions during embryogenesis and cancer progression. Cancer Science 98, 1512–1520.

63. Myers, 2000. Structure of the adult prostate from a clinician's standpoint. Clinical anatomy (New York, N.Y.) 13, 214–5.

64. Nguyen, AV, Pollard, JW, 2000. Transforming growth factor beta3 induces cell death during the first stage of mammary gland involution. Development.

65. Nobes, C.D., Hall, A., 1995. Rho, rac, and cdc42 GTPases regulate the assembly of multimolecular focal complexes associated with actin stress fibers, lamellipodia, and filopodia. Cell 81, 53–62.

66. Orton, K.C., Ling, J., Waskiewicz, A.J., Cooper, J.A., Merrick, W.C., Korneeva, N.L., Rhoads, R.E., Sonenberg, N., Traugh, J.A., 2004. Phosphorylation of Mnk1 by caspase-activated Pak2/gamma-PAK inhibits phosphorylation and interaction of eIF4G with Mnk. J. Biol. Chem. 279, 38649–57.

67. Papachristou, DJ, Basdra, EK, 2012. Bone metastases: molecular mechanisms and novel therapeutic interventions. Medicinal Research Reviews 32, 611-636.

68. Pasche, B., 2001. Role of transforming growth factor beta in cancer. J. Cell. Physiol. 186, 153–68.

69. Principe, Doll, Bauer, Jung, Munshi, Bartholin, Pasche, Lee, Grippo, 2014. TGF- : Duality of Function Between Tumor Prevention and Carcinogenesis. Jnci J Natl Cancer Inst 106, djt369–djt369.

70. Radu, M., Semenova, G., Kosoff, R., Chernoff, J., 2014. PAK signalling during the development and progression of cancer. Nature Reviews Cancer 14, 13–25.

71. Raftopoulou, Myrto., Hall, Alan., 2004. Cell migration: Rho GTPases lead the way. Develomental Biology 265, 23-32.

72. Rane, CK, Minden, A, 2014. P21 activated kinases: structure, regulation, and functions. Small GTPases.

73. Rangwala, R., Banine, F., Borg, J.-P., Sherman, L.S., 2005. Erbin regulates mitogen-activated protein (MAP) kinase activation and MAP kinase-dependent interactions between Merlin and adherens junction protein complexes in Schwann cells. Journal of Biological Chemistry 280, 11790–11797.

74. Renkema, GH, Pulkkinen, K, 2002. Cdc42/Rac1-mediated activation primes PAK2 for superactivation by tyrosine phosphorylation. Molecular and Cellular Biology 22, 6719-6725.

75. Ridley, A.J., Paterson, H.F., Johnston, C.L., Diekmann, D., Hall, A., 1992. The small GTP-binding protein rac regulates growth factor-induced membrane ruffling. Cell 70, 401–10.

76. Rong R, Surace EI, Haipek CA, Gutmann DH, Ye K., 2002. Serine 518phosphorylation modulates merlin intramolecular associationand binding to critical effectors important for NF2 growthsuppression. Oncogene 23, 8447–8454.

77. Rouleau GA1, Merel P, Lutchman M, Sanson M, Zucman J, Marineau C, Hoang-Xuan K, Demczuk S, Desmaze C, Plougastel B., 1993. Alteration in a new gene encoding a putative membrane-organizing protein causes neuro-fibromatosis type 2. Nature. 363, 515-521.

78. Rossi, MC., Zetter, BR., 1992. Selective stimulation of prostatic carcinoma cell proliferation by transferrin. PNAS. 89, 6197-6201.

79. Sathiakumar, N, Delzell, E, Morrisey, MA, 2011. Mortality following bone metastasis and skeletal-related events among men with prostate cancer: a population-based analysis of US Medicare beneficiaries, 1999–2006. Prostate Cancer and Prostatic Disease 14, 117-183.

80. Savagner, P., Yamada, K., Thiery, J., 1997. The Zinc-Finger Protein Slug Causes Desmosome Dissociation, an Initial and Necessary Step for Growth Factor β induced Epithelial to Mesenchymal Transition. J Cell Biology 137, 1403–1419.

81. Schiffer, M., Mundel, P., Shaw, A.S., Böttinger, E.P., 2004. A novel role for the adaptor molecule CDC42-associated protein in transforming growth factor β induced apoptosis. Journal of Biological Chemistry 279, 37004–37012.

82. Schroeder RD1, Angelo LS, Kurzrock R., 2014. NF2/merlin in hereditary neurofibromatosis 2 versus cancer: biologic mechanisms and clinical associations. Oncotarget. 5, 67-77.

83. Sheikh, S., Domin, J., Abel, P., Stamp, G., Lalani, E.-N., 2004. Phosphorylation of Both EGFR and ErbB2 Is a Reliable Predictor of Prostate Cancer Cell Proliferation in Response to EGF. Neoplasia 6, 846–853.

84. Siegel, R.L., Miller, K.D., Jemal, A., 2014. Cancer statistics, 2014. CA: a cancer journal for clinicians 65, 5–29.

85. Siu, M.K., Wong, E.S., Chan, H.Y., Kong, D.S., Woo, N.W., Tam, K.F., Ngan, H.Y., Chan, Q.K., Chan, D.C., Chan, K.Y., Cheung, A.N., 2010. Differential expression and phosphorylation of Pak1 and Pak2 in ovarian cancer: effects on prognosis and cell invasion. Int. J. Cancer 127, 21–31.

86. Sohn, E., 2015. Screening: Diagnostic dilemma. Nature 528, S120–S122.

87. Somanath, PR, Byzova, TV, 2009. 14-3-3β-Rac1-p21 activated kinase signaling regulates Akt1-mediated cytoskeletal organization, lamellipodia formation and fibronectin matrix assembly. Journal of cellular physiology.

88. Stattin, P., Vickers, A.J., Sjoberg, D.D., Johansson, R., Granfors, T., Johansson, M., Pettersson, K., Scardino, P.T., Hallmans, G., Lilja, H., 2015. Improving the Specificity of Screening for Lethal Prostate Cancer Using Prostate-specific Antigen and a Panel of Kallikrein Markers: A Nested Case-Control Study. Eur. Urol. 68, 207–13.

89. Takai, Y., Sasaki, T., Matozaki, T., 2001. Small GTP-Binding Proteins. Physiological Reviews 81, 153–208.

90. Tao, Y, Shen, C, Luo, S, Traoré, W, 2014. Role of Erbin in ErbB2-dependent breast tumor growth. Proceedings of the National Academi of Sciences. E4429-E4438.

91. Ueda, Y., Wang, S., Dumont, N., Yi, J.Y., Koh, Y., Arteaga, C.L., 2004. Overexpression of HER2 (erbB2) in human breast epithelial cells unmasks transforming growth factor β-induced cell motility. Journal of Biological Chemistry 279, 24505–24513.

92. Vanhaesebroeck, B., Waterfield, M.D., 1999. Signaling by distinct classes of phosphoinositide 3-kinases. Exp. Cell Res. 253, 239–54.

93. Vashchenko N, Abrahamsson PA, 2005. Neuroendocrine differentiation in prostate cancer: implications for new treatment modalities. European Urology. 47, 147–155.

94. Vleminckx, K, Vakaet, L, Mareel, M, Fiers, W, Roy, V.F., 1991. Genetic manipulation of E-cadherin expression by epithelial tumor cells reveals an invasion suppressor role. Cell.

95. Vogel, C, Marcotte, EM, 2012. Insights into the regulation of protein abundance from proteomic and transcriptomic analyses. Nature Reviews Genetics.

96. Wadman, M., 2015. Treatment: When less is more. Nature 528, S126–S127.

97. Wang, W., Zhou, G., Hu, M., Yao, Z., Tan, T.-H., 1997. Activation of the Hematopoietic Progenitor Kinase-1 (HPK1)-dependent, Stress-activated c-Jun N-terminal Kinase (JNK) Pathway by Transforming Growth Factor β (TGF-β)-activated Kinase (TAK1), a Kinase Mediator of TGF β Signal Transduction. J Biol Chem 272, 22771–22775.

98. Warner, D., Pisano, M.M., Roberts, E., Greene, R., 2003. Identification of three novel Smad binding proteins involved in cell polarity. Febs Lett 539, 167–173.

99. Webber, MM., Bello, D., Quader, S., 1997. Immortalized and tumorigenic adult human prostatic epithelial cell lines: characteristics and applications Part 2. Tumorigenic cell lines. Prostate. 30, 58-64.

100. Weir, K., 2015. Microbiology: Inflammatory evidence. Nature 528, S130–S131.

101. Wilkes, M., Mitchell, H., Penheiter, S., Doré, J., Suzuki, K., Edens, M., Sharma, D., Pagano, R., Leof, E., 2005. Transforming Growth Factor-β Activation of Phosphatidylinositol 3-Kinase Is Independent of Smad2 and Smad3 and Regulates Fibroblast Responses via p21-Activated Kinase-2. Cancer Res 65, 10431–10440.

102. Wilkes, M., Murphy, S., Garamszegi, N., Leof, E., 2003. Cell-Type-Specific Activation of PAK2 by Transforming Growth Factor β Independent of Smad2 and Smad3. Mol Cell Biol 23, 8878–8889.

103. Wilkes, M.C., Repellin, C.E., Hong, M., Bracamonte, M., Penheiter, S.G., Borg, J.-P.P., Leof, E.B., 2009. Erbin and the NF2 tumor suppressor Merlin cooperatively regulate cell-type-specific activation of PAK2 by TGF-beta. Develomental Cell 16, 433–44.

104. Wilkes, M.C., Stephen J., Nandor, Leo, E.B., 2003. Cell-Type-Specific Activation of PAK2 by Transforming Growth Factor b Independent of Smad2 and Smad3. Molecular and Cellular Biology 23, 8878–8889.

105. Xiao, GH, Beeser, A, Chernoff, J, Testa, JR, 2002. p21-activated kinase links Rac/Cdc42 signaling to merlin. Journal of Biological Chemistry 277, 883-886.

106. Xie, W, Mertens, JC, Reiss, DJ, Rimm, DL, Camp, RL, 2002. Alterations of Smad Signaling in Human Breast Carcinoma Are Associated with Poor Outcome A Tissue Microarray Study. Cancer research 62(2), 497-505.

107. Xu, J, Wang, R, Xie, ZH, Odero-Marah, V, Pathak, S, 2006. Prostate cancer metastasis: role of the host microenvironment in promoting epithelial to mesenchymal transition and increased bone and adrenal gland metastasis. The Prostate 66(15), 1664-1673.

108. Yan, X., Zhang, J., Sun, Q., Tuazon, P., Wu, X., Traugh, J., Chen, Y.-G., 2012. p21-activated Kinase 2 (PAK2) Inhibits TGF-β Signaling in Madin-Darby Canine Kidney (MDCK) Epithelial Cells by Interfering with the Receptor-Smad Interaction. J Biol Chem 287, 13705–13712.

109. Yang, J, Weinberg, RA, 2008. Epithelial-mesenchymal transition: at the crossroads of development and tumor metastasis. Developmental Cell 14(6), 818-829.

110. Yasuda, S, Oceguera-Yanez, F, Kato, T, Okamoto, M, 2004. Cdc42 and mDia3 regulate microtubule attachment to kinetochores. Nature 428, 767-771.

111. Yates, C, Shepard, CR, Papworth, G, Dash, A, 2007. Novel Three-Dimensional Organotypic Liver Bioreactor to Directly Visualize Early Events in Metastatic Progression. Advances in Cancer Research. 225-246.

112. Zayzafoon, M, Abdulkadir, SA, McDonald, JM, 2004. Notch signaling and ERK activation are important for the osteomimetic properties of prostate cancer bone metastatic cell lines. Journal of Biological Chemistry 279, 3662-3670.

113. Zhang, Y., Feng, X.-H., Wu, R.-Y., Derynck, R., 1996. Receptor-associated Mad homologues synergize as effectors of the TGF-β response. Nature 383, 168–172.

Appendices

A 1 - ERK Phosphorylation

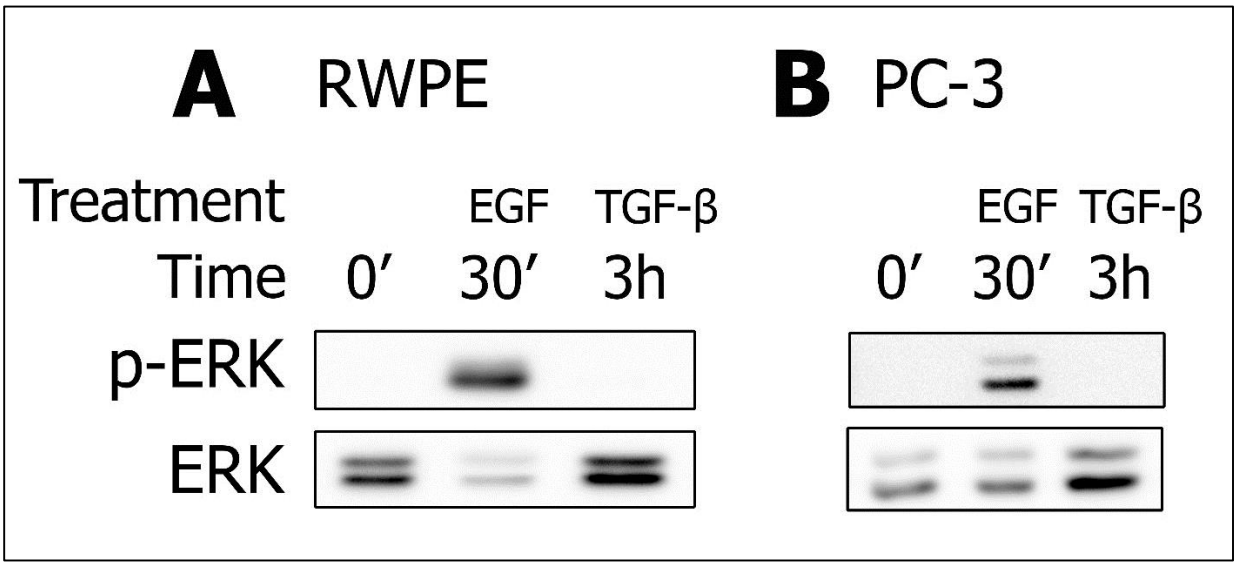

Figure A 1 - ERK phosphorylation in RWPE and PC-3 cells.

RWPE and PC-3 cells were treated with 100µg/ml of EGF and 5ng/ml of TGF-β to confirm ERK phosphorylation.

A 2 - DU145 Cell Migration

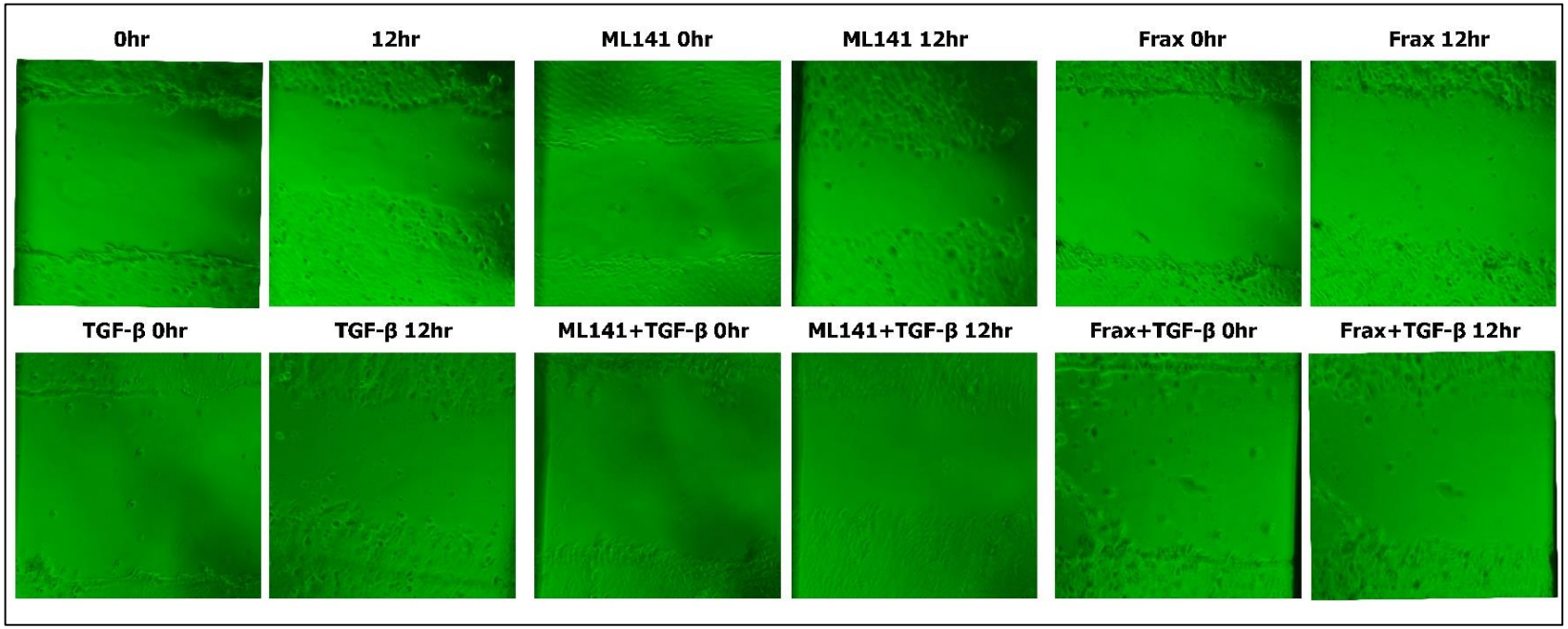

Figure A 2 - DU145 migration in the presence of TGF-β, ML141 and Frax1036

A 3 - PC-3 Cell Migration

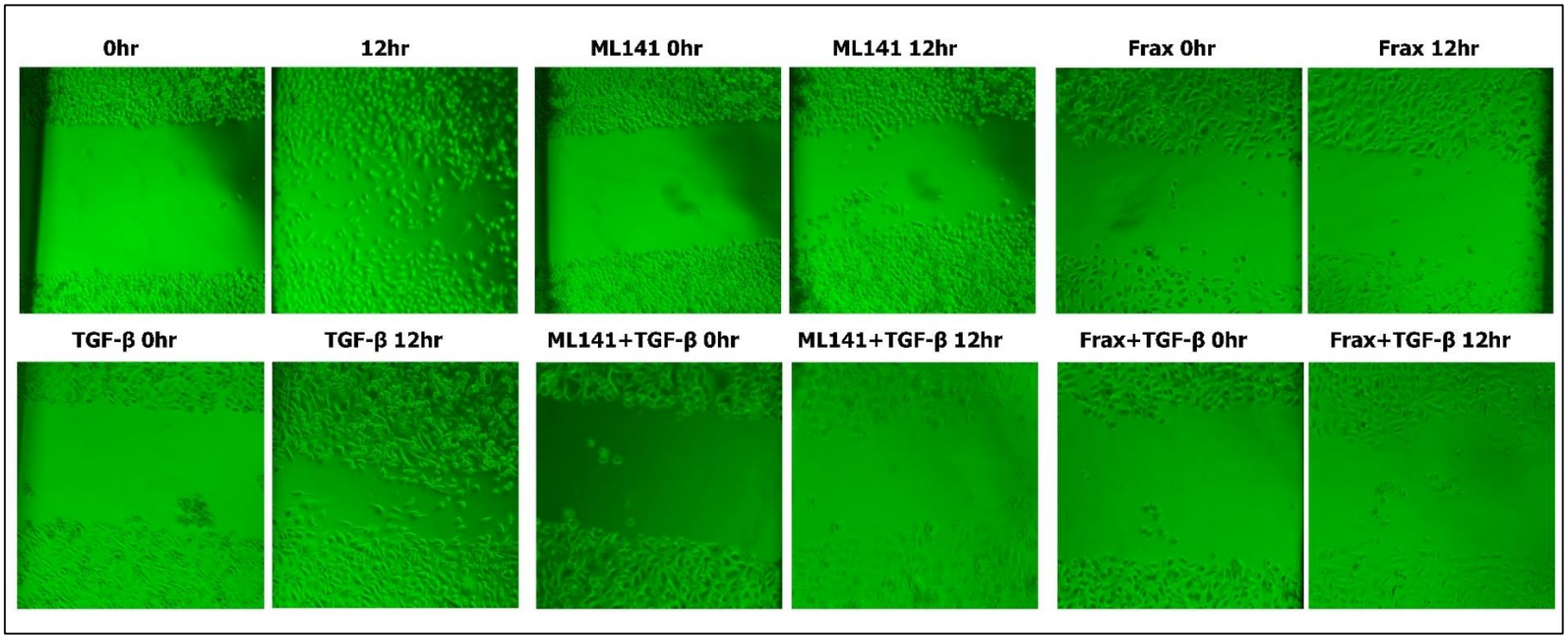

Figure A 3 – PC-3 migration in the presence of TGF-β, ML141 and Frax1036

A 4 - RWPE-1 Cell Migration

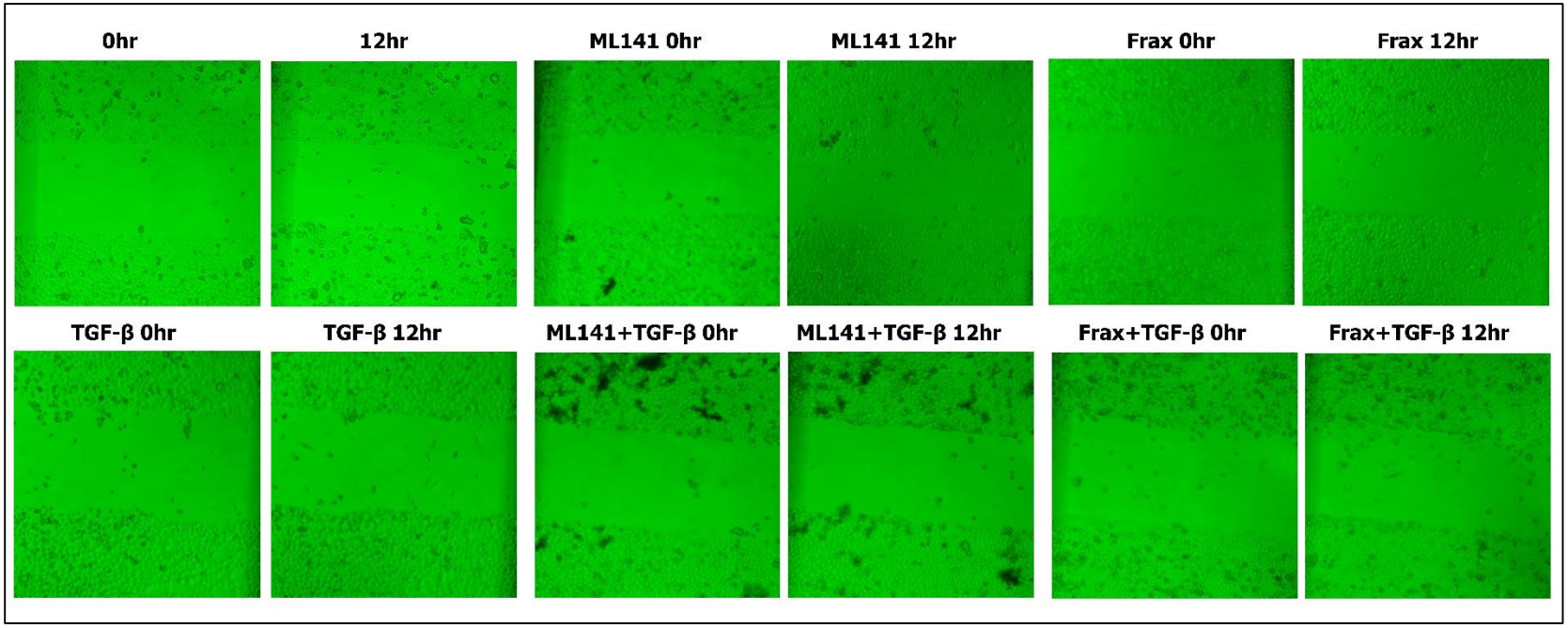

Figure A 4 – RWPE-1 migration in the presence of TGF-β, ML141 and Frax1036